A finite element analysis of 2D reactive flow

Corbey, R.M.

Award date:
1992

A finite element analysis of 2D reactive flow.

R.M. Corbey

Graduate report
TUE nr. WFW 92.015

Professor : Prof. dr. ir. H.E.H. Meijer
Coaches : Dr. ir. G.W.M. Peters
Dr. ir. F.N. van de Vosse

Eindhoven University of Technology (TUE)
Department of Mechanical Engineering
Division of Fundamental Mechanics
February 1992

Contents

Samenvatting

Het doel van dit onderzoek is modelvorming van reactieve stromingen (2D) en vervolgens numerieke simulatie van dit soort stromingen voor reële materialen. Voor het oplossen van de niet-lineaire gekoppelde vergelijkingen die het probleem beschrijven, is gebruik gemaakt van de eindige elementen methode. Deze methode kan worden toegepast in complexe twee dimensionale geometriën en is relatief eenvoudig uit te breiden tot een drie dimensionale omgeving. De modelvorming en numerieke oplosprocedure zijn getest aan de hand van voorbeelden met een bekende oplossing en simulatie van periodieke pijpstroming met gevulde epoxy. De experimenteel verkregen deformatie patronen van deze pijpstroming kunnen zichtbaar worden gemaakt en indien de chemische reaktie tijdens stroming klein is ten opzichte van de convectie van materiaal, zoals bij de beschreven simulaties het geval is, kunnen deze patronen worden vergeleken met de isoconversie lijnen uit de simulaties. Het blijkt dat de toegepaste oplosstrategie bruikbare resultaten oplevert. De conversie heeft een overheersende invloed op het snelheidsveld. De oplossing van de conversie vergelijking vertoont numerieke oscillaties in het gebied rond de hoekpunten.
Om publicatie van de resultaten mogelijk te maken is dit verslag geschreven in de vorm van een artikel met appendices.

A finite element analysis of 2D reactive flow

R.M. Corbey
Eindhoven University of Technology
Department of Mechanical Engineering

14 February 1992

Abstract

In this paper a numerical simulation of reactive flow is presented. The finite element method is employed to solve the governing coupled equations. The model is applied to a piston driven thermoset flow in a 2D rectangular cavity. The conversion of the material appears to have a decisive influence on the velocity field. The convection near the driving piston of material with conversion below and above the gelpoint is described quite well. The region near the cornerpoint at the wall and driven piston, shows substantial disturbance of the conversion field. The decoupling of equations by treating the right hand sides explicitly, proves to be useful.

Introduction

Reactive flow

Although numerous studies have been devoted to numerical solutions of flow problems in polymer processing, numerical simulations involving reactive flow are scarce and restricted to 2D problems or so-called $2\frac{1}{2}$D modelling. These models combine the finite difference and finite element method, see also [12]. Due to the complexity of solving a system of non-linear coupled partial differential equations incorporating complex material properties , it is not easy to provide accurate and efficient simulations. Yet, because of the increasing importance of predicting processes like R.I.M. , IC-packaging, compression moulding and the progress that has been made in computing capacity, the mathematical treatment of thermoset flow has gained in interest. In this paper a model is proposed for the simulation of two-dimensional flow of reactive material.
In the case of reactive flow, four equations have to be solved. Next to the mass-, impuls- and energy balance the conversion of reactive species yields a fourth balance. As predicting the conversion field implies precise knowledge of the "history" of the flow, it is essential to compute an accurate velocity profile.
The chemical reaction of the flow results in changing reaction rate, heat production and changing physical properties. Thermally induced polymerization and crosslinking are by nature instationary processes. This results in a system of unsteady equations. For the solution of these equations a finite element method was employed which is able to deal with complex 2D geometries and is relatively easy to extend to a three dimensional environment.

Significance

The model proposed in this paper, aimes at simulating reactive flow. To illustrate the purpose of these simulations a few examples are given of processes involving reactive flow.
The packaging of micro electronic devices is a thermoset polymer processing technology that requires high productivity and precision. In this area transfer molding has assumed an important role [9]. A compressed powder charge known as the preform is preheated above the glass transition temperature and inserted in a transfer pot. Subsequent a transfer ram pushes the preform towards a heated surface, forcing the material to flow into a number of runners to the mold cavities. The flow is in general three dimensional, also in the molds. The viscosity of the material depends upon temperature, shear rate and extent of chemical reaction. A high preheat temperature provides lower initial viscosities but higher reaction rate which subsequently increases the viscosity.
The design of transfer pot and runners dictates the imposed temperature and flow time; it is important to achieve the correct values because these determine the thermal history of a fluid particle. A study of reactive flow provides insight that can be used to optimize the transfer molding process. Moreover if it is possible to determine the flow behaviour of a particle, it is also possible to predict the starting position of this particle once the final position is known. This knowledge is essential when multi-component material is to be used.

Reaction injection molding (R.I.M.) implies the injection of a mixture of reactants into a mold where the material cures [4]. While filling the mold it has been recognized that material flowing near the midplane of the mold will advance faster than the flow front itself. This introduces the so called "fountain flow"; particles that are initially located near the center will move towards the wall when they enter the flow front region. The assumption that material particles can be considered to have straight path lines, is no longer valid.

In compression molding the charge , often consisting of a thermoset matrix holding reinforcing fibres, is placed in a mold after being preheated [6]. The upper half of the mold moves downward forcing the charge in its final shape. Next the charge cures in the mold. Because only small deformations occur this technique offers advantages especially when producing long-fibre reinforced materials.
The properties of the composite product are strongly affected by processing, the flow of the charge influences orientation and distribution of the fibres. Although flow will usually take place during the dwell time of the thermoset, the time span where cure is negligible, to produce the curing behaviour of the slab it is again crucial to find its temperature history as it flows in the mold.

The objective of the study reported in this paper is to model the flow of reactive material and to incorporate this model in the finite element package Sepran [11].
Of interest are the velocity, temperature and conversion fields that occur during thermoset flow. The model allows large Reynolds numbers to occur as is the case for R.I.M. Nylon [8]. Because properties of thermosets can vary greatly and are complex, it has been made possible to describe these material properties as functions of the independent

variables in an arbitrary way. In order to compare the simulations with experiments, to evaluate various aspects of thermoset flow as described before and because the main application of the modelling developed is the simulation of the IC-packaging process, a piston driven flow of an epoxy compound is studied in this paper.

Theory

Assuming that body forces are negligible, the equations of change which governs unsteady, incompressible fluid flow dynamics are :

$$\rho\dot{\vec{v}} + \vec{\nabla}p = \vec{\nabla}\cdot\boldsymbol{\sigma}^d \quad (1)$$

$$\vec{\nabla}\cdot\vec{v} = 0 \quad (2)$$

where ρ is the density, $\vec{v}$ is the velocity, p is the pressure and $\boldsymbol{\sigma}^d$ is the deviatoric part of the stress tensor. The balance of energy with constant thermal conductivity reads :

$$\rho C_p\dot{T} - \lambda\vec{\nabla}^2T = \boldsymbol{\sigma}^d : \mathbf{D} - H_r\frac{R}{C_0} \quad (3)$$

here C_p denotes the heat capacity, T is the temperature, λ is the thermal conductivity, $\mathbf{D}$ is the rate of strain tensor, H_r is the heat of reaction, R denotes the reaction rate and C_0 is the initial concentration of reactive species. The material balance on reactive species becomes :

$$\dot{C} - D\nabla^2C = -R \quad (4)$$

with C the concentration of reactive species and D the molecular diffusion coefficient. Or in terms of chemical conversion :

$$\dot{X} - D\nabla^2X = \frac{R}{C_0} \quad (5)$$

with X the extent of reaction (conversion). See also appendix A. For the description of the reaction kinetics of epoxy compound a phenomenologic equation is chosen. A model which has proved useful was proposed by Kamal and Sourour [7]. The rate of conversion is given by :

$$\frac{R}{C_0} = (K_1 + K_2X^m)(1-X)^n \quad (6)$$

The temperature dependence of the reaction rate is incorporated by K_1 and K_2:

$$K_1 = k_1exp(\frac{-\triangle E_1}{RT}) \quad (7)$$

$$K_2 = k_2exp(\frac{-\triangle E_2}{RT}) \quad (8)$$

$\triangle E_1$, $\triangle E_2$, m and n are constants following from experiments. For further information the reader is referred to appendix C and Spoelstra et.al.[13].
The material is assumed to behave as a generalized Newtonian fluid for which the viscosity is assumed a function of temperature, conversion and shear rate:

$$\eta = A_\eta(X) exp(\frac{E_\eta(X)}{RT})(2\mathbf{D} : \mathbf{D})^{\frac{n(X)}{2}} \tag{9}$$

$A_\eta(X)$,$E_\eta(X)$ and $n(X)$ depend upon conversion. See also appendix C and Spoelstra et.al.[13]. For $X = X_{gel}$ the viscosity is assumed to go to infinity. Assuming a generalized Newtonian behaviour the deviatoric part of the stress tensor, $\boldsymbol{\sigma}^d$, can be defined as :

$$\boldsymbol{\sigma}^d = 2\eta\mathbf{D} \tag{10}$$

where η is the viscosity as described by (9). Further assumptions are ;

1. Constant thermal properties (λ, C_p). This is not essential for the proposed model. The properties may be described as functions of any given variable.
2. Negligible molecular diffusion. The mass transfer Peclet number for the material involved is very large ($Pe_m = 10^8$). Therefore molecular diffusion can be neglected. See [2] and appendix A.
3. Constant heat of reaction (H_r). However, H_r can be implemented as a function of any given variable.
4. In order to approach solid material behaviour, the viscosity for conversion beyond gelpoint is set to a finite value, ten times the value as given by (9) for $X = X_{gel}$.

Numerical method

To solve the system of non-linear coupled partial differential equations, the finite element package Sepran is employed [11]. The velocity field is calculated using enriched quadratic triangles which satisfy the velocity-, pressure compatibility condition [5]. The energy and conversion balances are discretized using quadratic triangles. This leaves us with a system of four coupled equations. The equations are coupled by their right hand sides and the convection terms. Uncoupling is provided by treating these terms explicitly. In order to avoid partial pivoting, the equations of momentum and mass are uncoupled with the penalty function method [5]. This results in the following momentum and mass balance :

$$\rho\dot{\vec{v}} - \vec{\nabla}\frac{1}{\epsilon}\vec{\nabla}\cdot\vec{v} = \vec{\nabla}\cdot\boldsymbol{\sigma}^d \tag{11}$$

$$\epsilon\, p = -\vec{\nabla}\cdot\vec{v} \tag{12}$$

With sufficiently small ϵ the solutions of (11) and (12) approach the solutions of the original equations (1) and (2).

To approximate the time derivatives a Euler implicit method is used [15]. The solution strategy consists of solving each of the three equations at time level $n+1$, using the right hand side and velocity in the convection term calculated at the previous time level n. The time step between two successive solutions is assumed to be so small that iterations per time step are unnecessary. This strategy finally leads to the following sequence of discrete equations for each timestep :

For the whole domain at $t = 0$:
$\underline{U} = \underline{0}$, $\underline{T} = \underline{T_0}$, $\underline{X} = \underline{0}$.
For $t > 0, t_{end}$:

$$t^{n+1} = t^n + \Delta t$$

$$M_u \quad \frac{\underline{U}^{n+1} - \underline{U}^n}{\Delta t} + \frac{1}{\epsilon} L^T M_p^{-1} L \underline{U}^{n+1} = S_u(\underline{U}^n, \underline{T}^n, \underline{X}^n) \tag{13}$$

$$\epsilon M_p \quad \underline{P}^{n+1} = -L\underline{U}^{n+1} \tag{14}$$

$$M_T \quad \frac{\underline{T}^{n+1} - \underline{T}^n}{\Delta t} + N_T(\underline{U}^n)\underline{T}^{n+1} + K_T\underline{T}^{n+1} = F_T(\underline{U}^n, \underline{T}^n, \underline{X}^n) \tag{15}$$

$$M_X \quad \frac{\underline{X}^{n+1} - \underline{X}^n}{\Delta t} + N_X(\underline{U}^n)\underline{X}^{n+1} = F_X(\underline{U}^n, \underline{T}^n, \underline{X}^n) \tag{16}$$

where M_u denotes the velocity mass matrix, M_p is termed the pressure mass matrix, L represents the continuity equation, S_u denotes the stress matrix and the boundary conditions of the momentum equation. M_T denotes the energy mass matrix, N_T represents the convective terms in the energy equation, K_T is the heat conduction matrix and F_T is the discretization of the heat sources. M_X denotes the conversion mass matrix, N_X represents the convective terms in the conversion equation and F_X is the discretization of the reaction terms.

Because of the small molecular diffusion, the diffusion in equation (5) is neglected and equation (5) reduces to a first order partial differential equation. This may lead to oscillations in the solution. This behaviour can be suppressed by upwinding techniques. In the case of streamline upwinding an artificial diffusion is introduced in the direction of the streamlines. This way the extra error, as a result of upwinding, is restricted to this direction only [3]. However, the justification for such an approach is merely numerically founded, it is not guided by physical considerations.

Results

viscous heating

In order to study the behaviour of the uncoupling procedure as described in the previous section, first a relatively simple non-reactive problem is solved for which a solution is available. The problem consists of the non-isothermal flow of a power law fluid in a straight circular tube. The tube with radius and length of $4 * 10^{-1}$ and $1.3 * 10[mm]$, is discretized by a $8 * 10$ element mesh. Viscous heating is included but the viscosity is assumed to be temperature independent.

Fig. (1) shows the various temperature profiles in the constant wall temperature case. Next to the results derived with the finite element method, the figure also shows temperatures as presented by Bird and Armstrong from an analytical solution[1].See also appendix E. These temperatures have been computed by means of seperation of variables. As may be seen the results agree well.

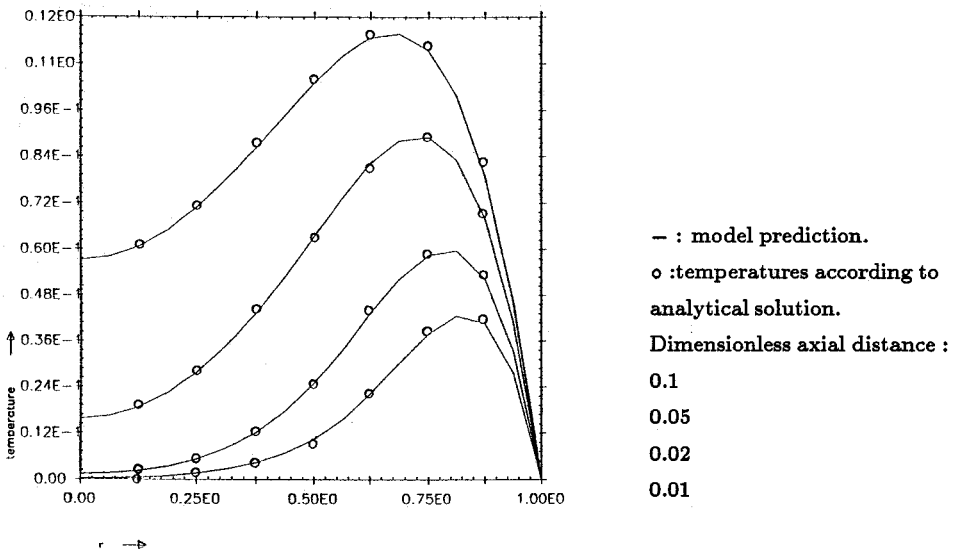

Figure 1: Temperature profiles in the constant wall temperature case for tube flow with viscous heating .

piston driven flow

Experiments and simulations with piston driven thermoplastics have been carried out by Vos et.al.[14]. Following on his work the curing and flow behaviour of piston driven and driving flow of thermoset material, has been simulated. This is a suitable case to study reactive flow because it encloses fountain flow and reverse fountain flow aswell as a stagnant zone. Moreover it is possible to validate the simulations with simple experiments by means of visualisation of deformation patterns [10]. These patterns will not be presented in the simulations as the particle tracking algorithm was not implemented in the program at the time.

The geometry that is dealt with consists of a $60 * 16[mm]$ rectangular cavity with two moving pistons : one driving the thermoset, the other one driven by it. To simplify

the problem the wall is assumed to move instead of the pistons. Moreover a no-slip condition holds on all boundaries. Since the conditions at the walls are identical, only half the part is considered. The mesh that is used consists of 1003 nodal points. It is shown in fig. (2). Notice that the plot has been scaled with factor 5 in cross direction.

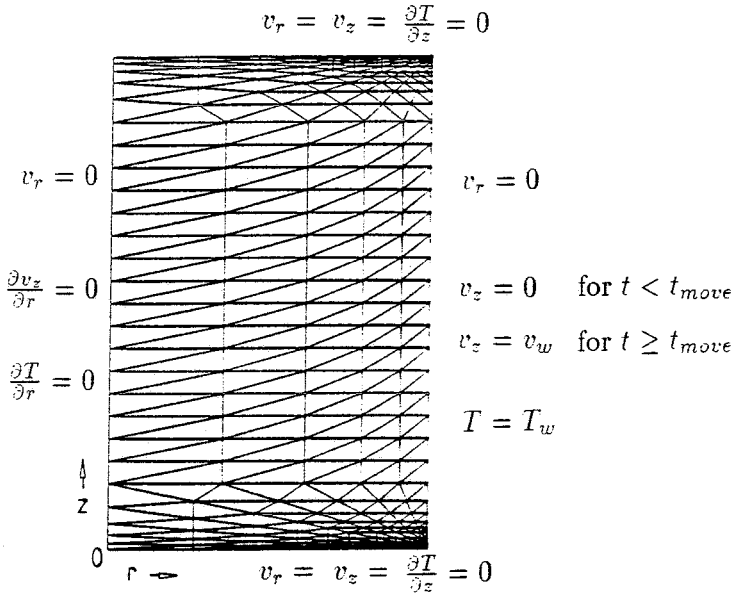

Figure 2: Element mesh with z-coordinate along the cavity and r-coordinate in cross direction

The thermoset is situated in a cavity of which the wall is kept at a constant temperature. The pistons are taken to be thermally insulated to provide a one dimensional problem as long as there is no movement. However this condition can be changed without any problem if this is advisable in view of more realistic boundary conditions. So boundary conditions are :

Driven piston	$v_r = 0$	$v_z = 0$	$\frac{\partial T}{\partial z} = 0$
Solid wall	$v_r = 0$	$v_z = 0$ for $t < t_{move}$	$T = T_w$
		$v_z = v_w$ for $t \geq t_{move}$	
Driving piston	$v_r = 0$	$v_z = 0$	$\frac{\partial T}{\partial z} = 0$
Midplane	$v_r = 0$	$\frac{\partial v_z}{\partial r} = 0$	$\frac{\partial T}{\partial r} = 0$

where v_w denotes the velocity at the wall and T_w the wall temperature. The initial conditions for the whole domain are :

$$T = 293[K] \quad (17)$$
$$X = 0 \quad (18)$$
$$\vec{v} = \vec{0} \quad (19)$$

Before the wall starts moving at $t = t_{move}$, the thermoset is heated for a periode in order to reach an extent of reaction that is high enough to influence the velocity

field. As this reaction takes place very slowly for the temperatures considered here and noticeable heat production due to reaction occurs for high conversion only, a timespan characteristic for the process is the cure time at the wall ; t_r. The timespan t_r is derived by integrating the reciprocal material balance (5) with $T = T_w$ and neglecting diffusion. See also appendix A and [6]. Because of the isothermal wall condition and the fact that $T_w > T_0$, a conversion field that changes drastically in the cross direction can be expected. Perpendicular to this direction, called the linear direction, this change will be considerably smaller. The reciprocal Damköhler II number that represents the diffusion-rate to reaction-rate ratio, is estimated to be 10^{-7}.

$$\frac{1}{DaII} = \frac{D\,t_r}{h^2} \tag{20}$$

If this ratio is raised a up to factor 10^6, reaction will still dominate diffusion. See also appendix A. Raising this ratio implies introduction of extra diffusion in the conversion equation. To avoid numerical oscillations in the conversion solution, streamline upwinding is introduced. This method implies adding extra diffusion to the convection diffusion equation in the direction of the streamlines. See also [3] and appendix B . Table (1) gives the values that have been used for the chemical system. These parameters were obtained from [13] and are representative for an epoxy compound applied for IC-packaging.

C_p	$1.8 * 10^3$	$[\frac{J}{kg\,K}]$
λ	$3 * 10^{-1}$	$[\frac{W}{m\,K}]$
k_1	$1.18 * 10^6$	$[\frac{1}{s}]$
k_2	$4.71 * 10^7$	$[\frac{1}{s}]$
$\triangle E_1$	$70.1 * 10^3$	$[\frac{J}{mol}]$
$\triangle E_2$	$74.1 * 10^3$	$[\frac{J}{mol}]$
n	1.38	$[-]$
m	1.24	$[-]$
ρ	$1.2 * 10^3$	$[\frac{kg}{m^3}]$
X_{gel}	$1.8 * 10-1$	$[-]$
H_r	$-9 * 10^7$	$[\frac{J}{m^3}]$

Table 1: *Thermal and kinetic parameters*

The viscosity was fitted using nineth order polynomals. See appendix C and [13]. In order to limit the displacement of the material so deformations are still interpretable, the velocity of the wall was taken to be $v_w = 2.5 * 10^{-3}[\frac{m}{s}]$ for a timespan of $8[s]$ in all cases. The start of the wall movement was set to $t_{move} = 300[s]$, in the preceding period the thermoset is heated with an isothermal wall temperature T_w. These settings are in agreement with experiments carried out by Schouenberg [10]. Fig. (3) shows the conversion profiles of the thermoset charge at various points in time for a wall temperature of $T_w = 384[K]$.

The profiles are taken halfway the cavity length. Because of the no-slip condition at the boundaries and the constant temperature , the thermal history of the material

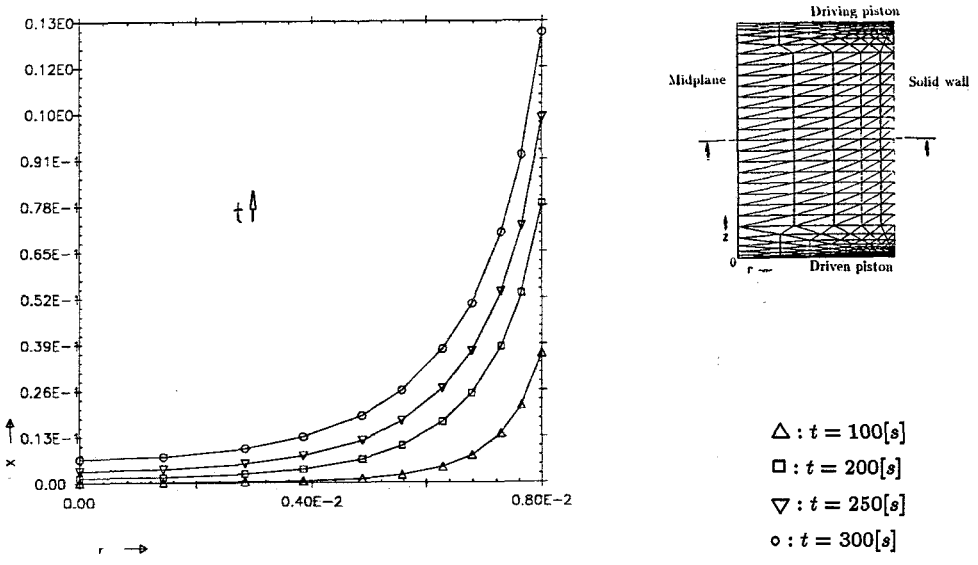

Figure 3: Extent of reaction from midplane to wall of the cavity at various times. $T_w = 384[K]$.

points at the wall is known. Therefore the extent of reaction can be computed by integrating equation (6) with $T = T_w = 384[K]$ for material that remains at the wall during movement. In this way the numerical results shown in fig. (3) can be checked. The results are presented in table (2).

$t[s]$	$X_w[-]$
100	0.037
200	0.079
250	0.103
300	0.128

Table 2: *Extent of reaction at the wall.* $T_w = 384[K]$.

The values compare good to those presented in fig. (3). There's a sharp rise in extent of reaction at the wall. Since there is very little heat generated due to chemical reaction, the extent of reaction near the center of the part remains small. The conversion is well below the gelpoint which is at $X = 0.18$. Fig. (4) shows the temperature profiles for the same example.
The imposed wall temperature is not exceeded, so it is clear that conduction outweighs reaction heat . This is indicated by the Damköhler IV number which represents the ratio of rates of temperature rise due to reaction and conduction ;

$$DaIV = \left| \frac{h^2 \, H_r}{(T_w - T_0) \, t_r \, \lambda} \right| \tag{21}$$

If the characteristic reaction time t_r is defined according to [6] as the cure time at the wall, then the Damköhler IV number becomes ;

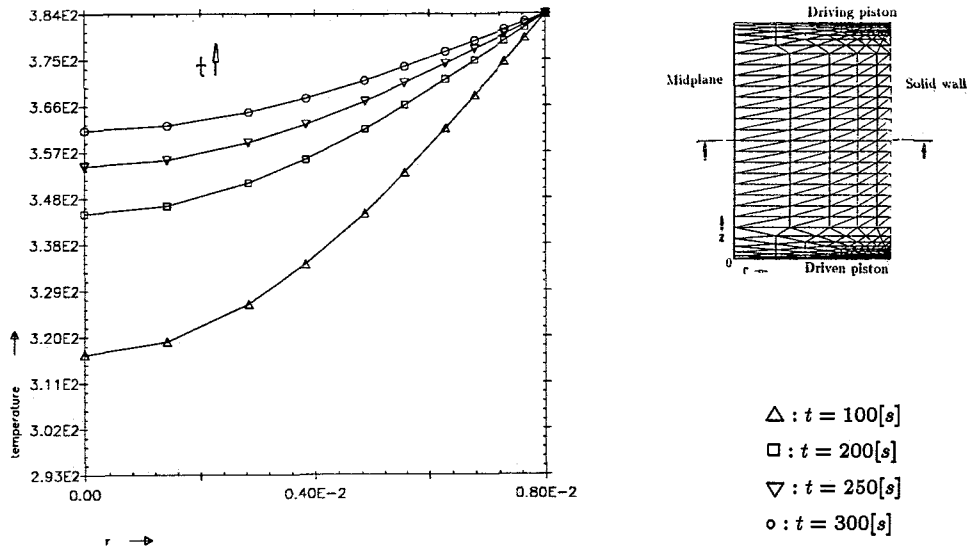

Figure 4: Temperature from midplane to wall of the cavity at various times.

$$DaIV = 0.21 \tag{22}$$

See also appendix A. Fig. (5) shows the velocity field at $t = 308[s]$ and the velocity in cross direction at intersection $r = 4[mm]$ at various times.
The material approaches the driving piston along the wall. It then enters the reverse-fountain flow region, moves towards the midplane and is directed to the driven piston. The maximum velocity in linear direction is about four times the maximum velocity in the cross direction. During the time the wall is moving, the area where a velocity in cross direction is present, extends. The section where cross flow occurs, is bounded by the pistons and two turning points. In these turning points the velocity in either direction is zero. During the flowtime, the turning points move towards each other, enlarging the cross flow section. As the intersection shows, the enlargement of the cross flow section results in a less high and a wider velocity profile near the driving piston. Near the driven piston the development of the profile is more complicated. First the profile shows a large reduction in hight. The profile becomes flatter and developes two small peaks. Next, one of the peaks is seperated and the other peak increases its value. At $t = 308[s]$ the vector plot of velocity shows a cross flow section directed to the wall that covers half the cavity length. The cross flow section directed to the midplane occupies no more than a quarter of the cavity length. The maximal Reynolds number was found to be 10^{-6}. Fig. (6) shows the temperature distributions at $t = 300$, 304 and $t = 308[s]$.

Notice that the flow towards the heated wall causes a large temperature gradient near the cornerpoint at the driven piston. Material at the pistons will stick to it and the temperature at the piston walls is therefore only a result of diffusion and reaction. The wiggles that occur near the midplane and driving piston, are probably due to the mesh that is rather coarse here.
Fig. (7) describes the conversion fields at three points in time. It is clear that the lower part of this field is affected by non-physical oscillations. These oscillations occur mainly

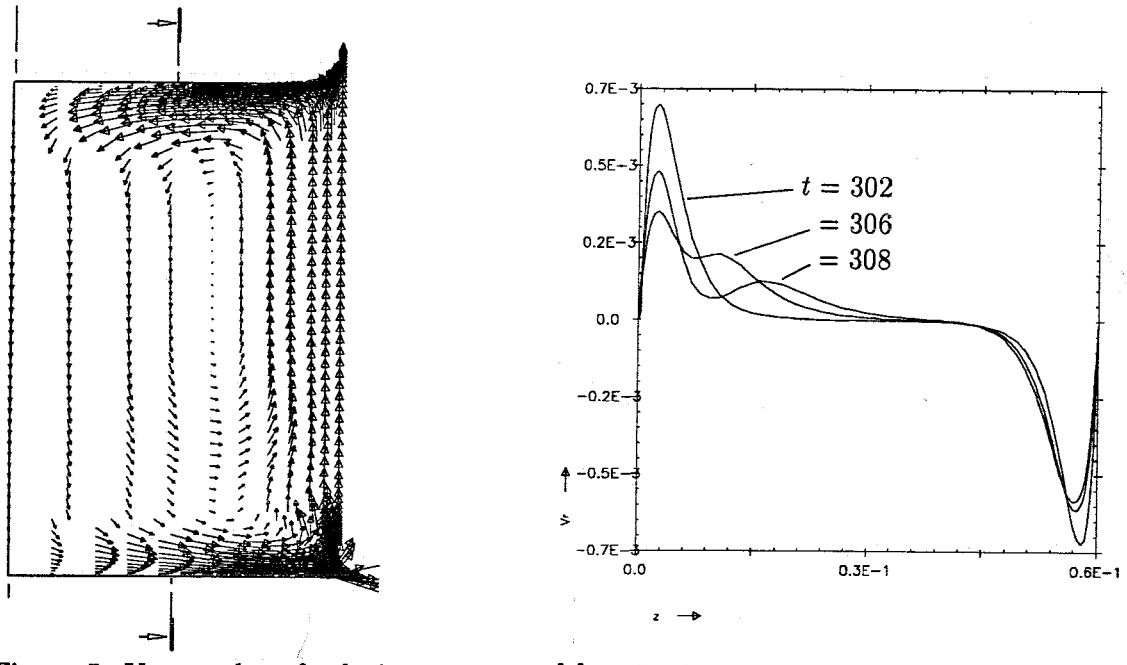

Figure 5: Vector plot of velocity at $t = 308[s]$ and velocity in cross direction at intersection $r = 4[mm]$ at $t = 302, 306, 308[s]$. $T_w = 384[K]$.

at the pistons and are transported to the wall and along the pistons. Because of the artificial diffusion in the conversion equation, these disturbances remain restricted to an acceptable area. The influence of the velocity distribution on the conversion field is evident. Due to the large area of cross flow towards the wall, a gradient of conversion in linear direction is visible near the heated wall over a substantial length. Contrary to the cross flow near the driving piston, where the material has a linear velocity component, the flow near the driven piston is pointed straight at the wall. This causes an extreme conversion gradient at the cornerpoint of the driven piston.

Next to a case with $T_w = 384[K]$, also a case with $T_w = 393[K]$ is considered. Moreover this problem is solved for non-reacting material in order to investigate heat production due to reaction and to compare velocity distributions. Fig. (8) shows the conversion profiles for $T_W = 393[K]$. The conversion at the wall is well beyond gelpoint. As a check the values at the wall can be compared with values obtained by integration of equation (6), listed in table (3). The difference in conversion at each time level is of order magnitude 10^{-3}. Fig. (8) also shows that during the timespan that the charge is moved, the conversion of reactive species is very small . This enables us to interpretate the contour levels of conversion as deformation lines and to compare them to experiments.

Fig. (9) illustrates the temperature distribution for $T_w = 393[K]$ for reactive and non-reactive material. The non-reacting temperature profile is only shown at $t = 308[s]$. There is practically no heat production due to chemical reaction, so the overall temperature stays below the wall temperature. The conversion is still too small to cause a temperature rise. Fig. (10) shows the velocity in linear direction for two different wall temperatures and a profile for the non-reacting case with wall temperature

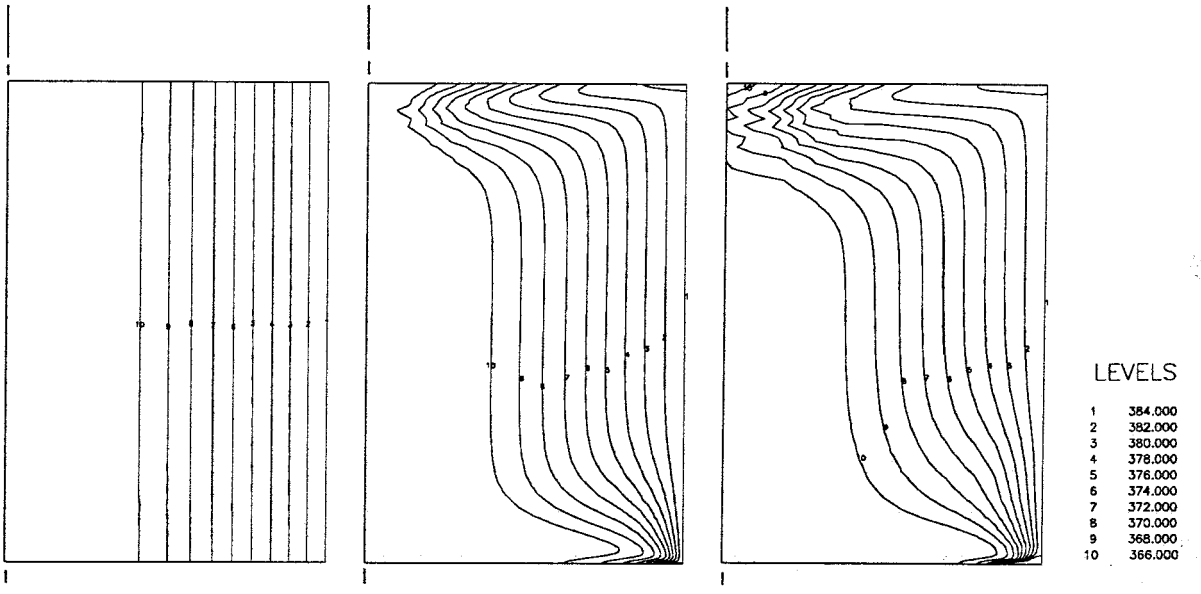

Figure 6: Contour levels of temperature. $T_w = 384[K], t = 300$, 304 and $308[s]$.

$t[s]$	$X_w[-]$
100	0.065
200	0.148
250	0.199
300	0.254
308	0.265

Table 3: *Extent of reaction at the wall.* $T_w = 393[K]$.

$T_w = 393[K]$. As may be seen the influence of the conversion is very large. Although the gelpoint hasn't been reached for $T_w = 384[K]$, the velocity is high at the wall. A higher wall temperature gives higher conversion values and therefore a higher viscosity. The influence on the viscosity by temperature is overruled by conversion. This accounts for the flatter velocity profile that appears for $T_w = 393[K]$ at the wall. If we compare these profiles with the respective temperature distributions, it can be noted that conversion beyond the gelpoint produces a layer of material that behaves like a solid; the velocity is that of the wall. The treatment of the viscosity for $X \geq X_{gel}$ appears to be useful. For the non-reactive example a flatter-than-parabolic profile is observed which is in agreement with shearthinning materials . The temperature distribution amplifies this behaviour.

Fig (11) shows the vector plot of velocity and two region plots at $t = 308[s]$. As may be seen the velocity distribution differs from the case with $T_w = 384[K]$. In the lower cross flow section the velocity profile is parabolic, similar to the upper cross flow section. The region plots show a thin layer of material that remains at the driven piston.

However the cause of this behaviour is probably the oscillating conversion which results in a high viscosity at the pistons.

Fig. (12) shows the isotherms before and after the wall starts moving for $T_w = 393[K]$. The conversion of the material reaches a considerable higher level than in the case of $T_w = 384[K]$. It has passed the gelpoint, therefore the material adjacent to the heated wall produces high viscous dissipation when it is forced to move from the wall to the driving piston, through the cornerpoint. The temperature rise due to the above dissipation is about $90[K]$.

Fig. (13) illustrates the conversion fields for $T_w = 393[K]$. The oscillation region is of the same size as for the lower temperature case. As fig. (10) shows, the velocity profile resambles a sharp "s" with the neutral line ($v_z = 0$) close to the midplane. As a result of this, the reversal flow near the midplane doesn't advance uniformly from the reverse fountain flow region through the cavity. It developes a peak. The high-velocity layer at the moving wall results in high velocities in the cross flow section. This is illustrated by the vector plot of velocity in fig. (11). It can be noted that the conversion has no prescribed value at the wall, so the movement of the iso-conversions should be in agreement with the prescribed velocity. Fig. (13) shows that this is actually the case, the iso-conversion nearest to the wall is transported $20[mm]$ in $8[s]$. This is equal to the wall movement. This behaviour also emphasizes that in this case, the chemical reaction that takes place during the 8 seconds of movement, can be neglected with respect to the convection of material. See also appendix A.

Experiments for a case similare to the simulations described in this paper were carried out by Schouenberg [10]. Fig. (14) shows the deformation patterns for a piston driven epoxy compound in a straight circular tube. The wall temperature is $T_w = 384[K]$. The preheat period is 5 minutes and the thermoset charge is moved for 8 seconds with a wall velocity of $2.5 * 10^{-3}[\frac{m}{s}]$. Although the experiments correspond to a circular domain and thus only qualitatively comparison is possible, the velocity field tends to the same shape as presented in fig. (10). The material near the wall has developed a uniform velocity and the deformation pattern in the center of the part is very narrow. Although heating from the wall in a tube takes place over a larger surface than in the case of a rectangular cavity, it is assumed that the conversion has not reached a substantial higher level in the tube. In view of this fact, the experiment and the simulations can be compared.

Conclusions and discussion

A model has been put forward that describes the coupled phenomena of flow, chemical reaction and heat transfer. The conversion and temperature field influence the viscosity and consequently the velocity field. The velocity affects the conversion and temperature fields by transport of material particles. When the conversion equation is solved by the finite element method, measures have to be taken to avoid numerical oscillations . In the study of piston driven material these problems arise in the region of the cornerpoints of the cavity. Especially near the cornerpoint of the driven piston, a region is created with large oscillations. The cornerpoint near the driving piston doesn't bring about this amount of disturbance. The limitation of oscillations has been provided effectively

by use of streamline upwinding.
The simulations have shown that a high wall temperature results in high conversion at the wall. If this conversion is above gelpoint, the movement of this material around the cornerpoint will cause an extreme temperature rise. If these temperatures would appear in a real thermoset, they would cause thermal degradation of the polymer. However, it can be questioned if flow around the corner would actually take place in an experiment with material above gelpoint at a moving wall. The possibility excists that the gel is detached from the wall and the complete charge, although not fully gelled, will advance uniform. The above can be a physical basis for the introduction of slip.
The decoupling of the equations, as far as their right hand sides and convective terms are concerned, proves to be effective. Although these terms are treated explicitly, they do not result in instable solutions. The derived conversion values at the wall, indicate that the proposed solution strategy is accurate. From the velocity profiles it can de concluded that setting the viscosity to a high finite value for gelled material, is a useful way of approximating solid material behaviour. For the examples presented, the reaction rate appears to be small. During the $8[s]$ of movement this chemical reaction is negligible compared to the convection of material. Therefore the iso-conversion contourlines can be used to visualize the deformation process. Taking this into account the two considered wall temperatures provide a clear difference in deformation patterns. These deformations can be visualized by simple experiments as described in [14] and [10]. In this way the numerical results can be verified further.
The velocity field that occurs for $T_w = 384[K]$ shows a cross flow section towards the heated wall that developes two peaks. The mechanism of this behaviour is not known and needs to be studied further.

Aknowledgement- The author is grateful to Gerrit Peters and Frans van de Vosse for their contribution to this paper.

Notation

$A_\eta(X)$	=	pre-exponential factor in viscosity expression
C	=	concentration of reactive species
C_0	=	initial concentration of reactive species
C_p	=	heat capacity
D	=	molecular diffusion coefficient
$\mathbf{D}$	=	rate of strain tensor
$E_\eta(X)$	=	viscosity activation energy
η	=	viscosity
$\triangle E_1$	=	reaction activation energy
$\triangle E_2$	=	reaction activation energy
ϵ	=	penalty function parameter
h	=	cavity thickness
H_r	=	heat of reaction
$k1$	=	pre-exponential factor in kinetic constant
$k2$	=	pre-exponential factor in kinetic constant
K_1	=	kinetic rate constant
K_2	=	kinetic rate constant
λ	=	thermal conductivity
m	=	kinetic power index
n	=	kinetic power index
$n(X)$	=	viscosity power index
p	=	pressure
r	=	coordinate in cross direction
ρ	=	density
R	=	reaction rate
R	=	gas constant
$\boldsymbol{\sigma}^d$	=	deviatoric part of the stress tensor
t	=	time
t_r	=	characteristic reaction time
$\triangle t$	=	time step
T	=	temperature
T_w	=	wall temperature
T_0	=	initial material temperature
θ	=	parameter in theta-method
$\vec{v}$	=	velocity
v_r	=	velocity in cross direction
v_w	=	velocity at the wall
v_z	=	velocity in linear direction
X	=	extent of reaction
X_w	=	extent of reaction at the wall
z	=	coordinate in linear direction

Dimensionless numbers

$DaII$	=	Damköhler II number
$DaIV$	=	Damköhler IV number
Re	=	Reynolds number

References

[1] R.B Bird, R.C Armstrong and O. Hassager. *Dynamics of polymeric liquids, 1987*

[2] R.B. Bird, W.E. Stewart and E.N. Lightfoot. *Transport phenomena, 1960*

[3] A.N. Brooks and T.J.R. Hughes. *Comp.Meth.Appl.Mech.and Eng., 32 1982*

[4] E. Broyer and C.W. Macosko. *AIChE Journ. 22:2*

[5] C. Cuvelier, A. Segal and A.A. v. Steenhoven. *Finite element methods and Navier-Stokes equations, 1986*

[6] A.I. Isayev. *Injection and compression molding fundamentals, 1987*

[7] M.R. Kamal and S. Sourour. *Polym.Eng.Sci., 13:41 1976* and *Thermoch.Acta, 14:41 1976*

[8] C.W. Macosko. *Fundamentals of reaction injection molding, 1989*

[9] L.T. Manzione, G.W. Poelzing and R.C. Progelhof. *Polym.Eng.Sci., 28:16 1988*

[10] M.J.F.H. Schouenberg. *TUE report, WFW 91.003 1991*

[11] A. Segal *Sepran manual, 1989*

[12] C. Sitters. *Numerical simulation of injection moulding, 1988*

[13] A.B. Spoelsta and J.M.M. de Kok. *TUE report, WFW 91.059 1991*

[14] E. Vos, H.E.H. Meijer, G.W.M Peters. *Int.Pol.Proc., 6:1 1991*

[15] F.N. v.d. Vosse, A.A. v. Steenhoven, A. Segal and J.D. Janssen. *Int.J.Num.Meth.fluids, 6 1986*

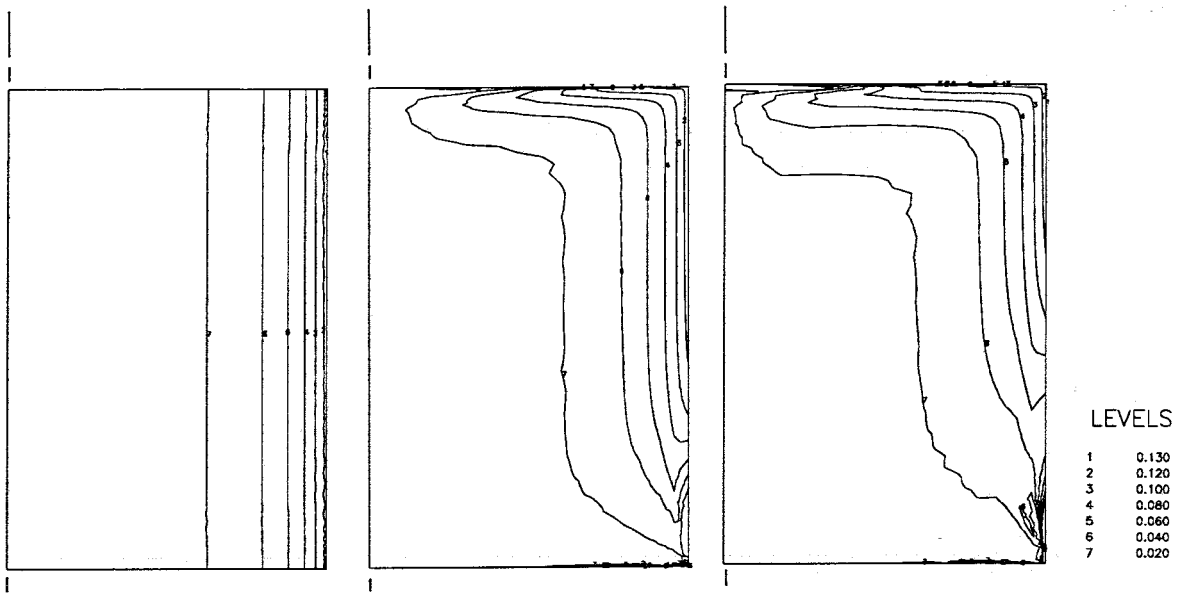

Figure 7: Contour levels of conversion. $T_w = 384[K], t = 300$, 304, and $308[s]$.

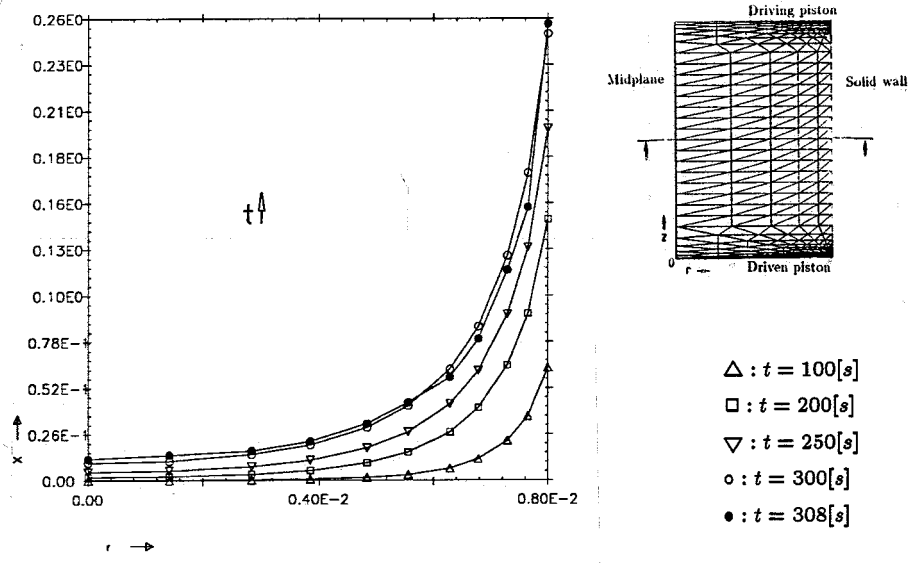

Figure 8: Extent of reaction from midplane to wall of the cavity. $T_w = 393[K]$.

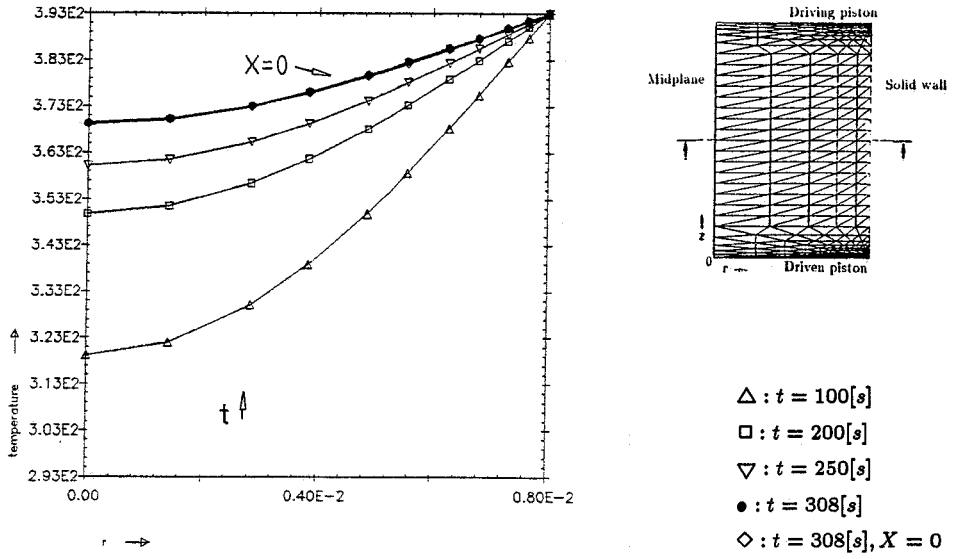

Figure 9: Temperature from midplane to wall of the cavity. $T_w = 393[K]$.Reactive and non-reactive.

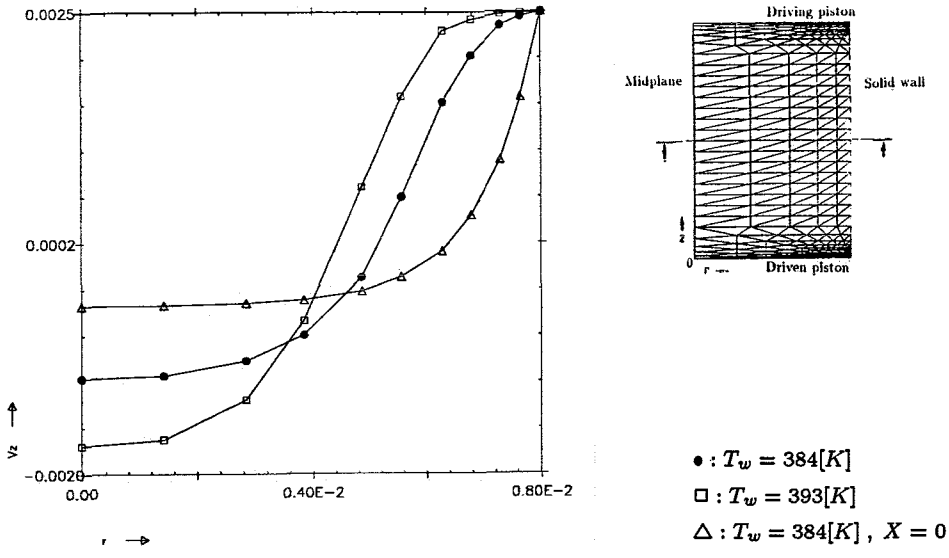

Figure 10: Velocity in linear direction, from midplane to wall of the cavity. $t = 308[s]$. Reactive and non-reactive.

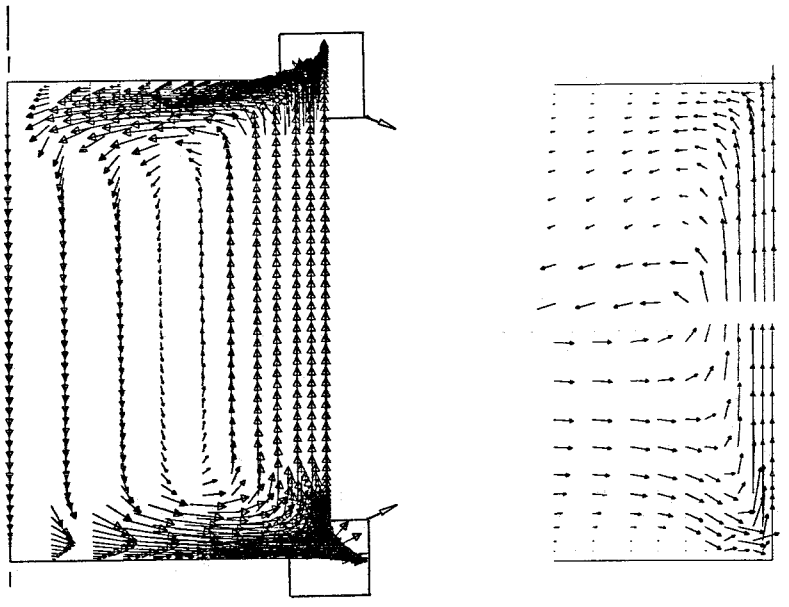

Figure 11: Vector plot of velocity and region plots near the cornerpoints . $T_w = 393[K], t = 308[s]$.

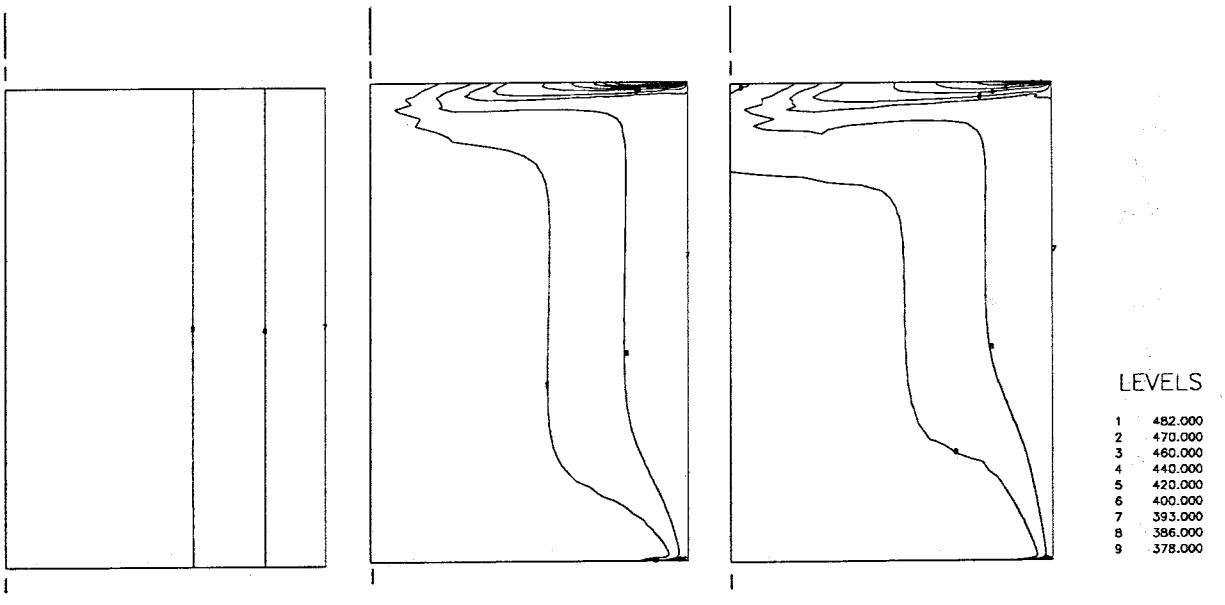

Figure 12: Contour levels of temperature. $T_w = 393[K], t = 300$, 304, and $308[s]$.

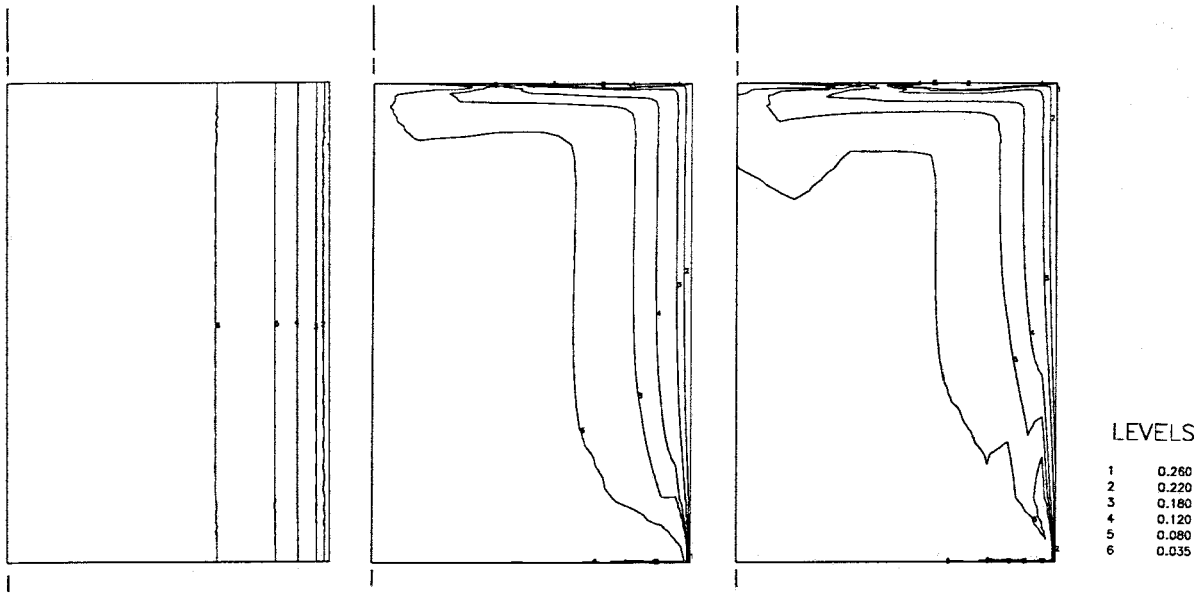

Figure 13: Contour levels of conversion. $T_w = 393[K], t = 300$, 304 and $308[s]$.

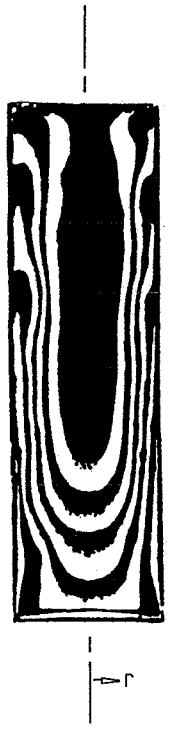

Figure 14: Deformation patterns in a straight circular tube according to Schouenberg . $T_w = 384[K], t = 308[s]$.

Appendix A

The balance equations

A.1 The energy balance

The balance of energy reads :

$$\rho \dot{u} = -\vec{\nabla} \cdot \vec{q} + \boldsymbol{\sigma} : \mathbf{D} + \rho r_r \tag{A.1}$$

where u is the specific internal energy and r_r is the specific radiation absorbed by the body.

A.1.1 Elimination of $\dot{u}$ from the Clausius Duhem inequality.

The Clausius Duhem inequality reads :

$$\rho T \dot{s} - \rho \dot{u} + \boldsymbol{\sigma} : \mathbf{D} - \frac{\vec{q} \cdot \vec{\nabla} T}{T} \geq 0 \tag{A.2}$$

The specific free energy is defined as :

$$f = u - Ts \tag{A.3}$$

where s is the specific entropy.
Choose for a compressible, conductive, viscous binary mixture, the following independent variables ;

ρ	=	density
$X = \frac{C_0 - C}{C_0}$	=	conversion
$\mathbf{L}$	=	$\vec{\nabla}\vec{v}$ (or $\dot{\rho}$ and $\mathbf{L}^d$)
T	=	temperature
$\vec{\nabla} T$	=	temperature gradiënt

This gives ;

$$f = f(\rho, \dot{\rho}, X, \mathbf{L}^d, T, \vec{\nabla} T) \tag{A.4}$$

Using :

$$\begin{aligned}\boldsymbol{\sigma}:\mathbf{D} &= \left[-p\,\mathbf{I}+\boldsymbol{\sigma}^d\right]:\mathbf{D}\\ &= -p\,tr(\mathbf{D})+\boldsymbol{\sigma}^d:\mathbf{D}\\ &= -p\,\dot{J}/J+\boldsymbol{\sigma}^d:\mathbf{D}\\ &= p\,(\dot{\rho}/\rho)+\boldsymbol{\sigma}^d:\mathbf{D}\end{aligned} \tag{A.5}$$

with $p=-\frac{1}{3}tr(\boldsymbol{\sigma})$ the Clausius Duhem inequality becomes ;

$$\dot{u}=\dot{f}+T\,\dot{s}+\dot{T}\,s \Rightarrow$$
$$-\rho\,(\dot{T}\,s+\dot{f})+(\dot{\rho}/\rho)\,p+\boldsymbol{\sigma}^d:\mathbf{D}-\frac{\vec{q}\cdot\vec{\nabla}T}{T}\geq 0 \tag{A.6}$$

As

$$\dot{f}=\left(\frac{\partial f}{\partial \rho}\right)\dot{\rho}+\left(\frac{\partial f}{\partial \dot{\rho}}\right)\ddot{\rho}+\left(\frac{\partial f}{\partial X}\right)\dot{X}+\left(\frac{\partial f}{\partial \mathbf{L}^d}\right)^c:\dot{\mathbf{L}}^d+\left(\frac{\partial f}{\partial T}\right)\dot{T}+\left(\frac{\partial f}{\partial \vec{\nabla}T}\right)\cdot\left(\vec{\nabla}\dot{T}\right) \tag{A.7}$$

(A.6) can be written as ;

$$-\rho\dot{T}\,s+\left(p/\rho-\rho\frac{\partial f}{\partial \rho}\right)\dot{\rho}-\rho\left(\frac{\partial f}{\partial \dot{\rho}}\right)\ddot{\rho}-\rho\left(\frac{\partial f}{\partial X}\right)\dot{X}-\rho\left(\frac{\partial f}{\partial \mathbf{L}^d}\right)^c:\dot{\mathbf{L}}^d-\rho\left(\frac{\partial f}{\partial T}\right)\dot{T}$$
$$-\rho\left(\frac{\partial f}{\partial \vec{\nabla}T}\right)\cdot\left(\vec{\nabla}\dot{T}\right)+\boldsymbol{\sigma}^d:\mathbf{D}-\frac{\vec{q}\cdot\vec{\nabla}T}{T}\geq 0 \tag{A.8}$$

Determination of the independent variables implies that the derivatives of these variables can be chosen free (in our case $\ddot{\rho},\dot{\mathbf{L}}^d,\dot{T},\vec{\nabla}\dot{T}$).
As (A.8) has to be valid for an arbitrary combination of these derivatives, the following must be true :

$$\begin{aligned}\frac{\partial f}{\partial \dot{\rho}} &= 0\\ \frac{\partial f}{\partial \mathbf{L}^d} &= \mathbf{0}\\ \frac{\partial f}{\partial \vec{\nabla}T} &= \vec{0}\\ \text{and } s &= -\left(\frac{\partial f}{\partial T}\right)\end{aligned}$$

From (A.7) and the above equalities it can be concluded that :

$$f=f(\rho,T,X)\text{ and }u=u(\rho,T,X) \tag{A.9}$$

This reduces the Clausius Duhem inequality to :

$$1/\rho\left(p-\rho^2\frac{\partial f}{\partial \rho}\right)\dot{\rho}-\rho\left(\frac{\partial f}{\partial X}\right)\dot{X}+\boldsymbol{\sigma}^d:\mathbf{D}-\frac{\vec{q}\cdot\vec{\nabla}T}{T}\geq 0 \tag{A.10}$$

To eliminate p the thermodynamic pressure p_0 is introduced ;

$$p=p_0(\rho,T,X)+p_1(\rho,\dot{\rho},X,\mathbf{L}^d,T,\vec{\nabla}T) \tag{A.11}$$

with $p_0 \stackrel{\text{def}}{=} \frac{\partial f}{\partial \rho}\rho^2$. the Cauchy stress tensor becomes :

$$\begin{aligned}\boldsymbol{\sigma} &= -p\mathbf{I}+\boldsymbol{\sigma}^d \\ &= -p_0\mathbf{I}\underbrace{-p_1\mathbf{I}+\boldsymbol{\sigma}^d} \\ &= -p_0\mathbf{I}+\boldsymbol{\sigma}^e\end{aligned} \tag{A.12}$$

where $\boldsymbol{\sigma}^e$ is the so called extra stress tensor.Insertion of $\boldsymbol{\sigma}^d$ and the definition of $\frac{\partial f}{\partial \rho}\rho^2$, in (A.10) gives :

$$\begin{aligned}\dot{\rho}/\rho\underbrace{(p-p_0)}_{p_1}-\rho\left(\frac{\partial f}{\partial X}\right)\dot{X}+(\boldsymbol{\sigma}^e+p_1\mathbf{I}):\mathbf{D}-\frac{\vec{q}\cdot\vec{\nabla}T}{T} &\geq 0\Rightarrow \\ -tr(\mathbf{D})\,p_1-\rho\left(\frac{\partial f}{\partial X}\right)\dot{X}+(\boldsymbol{\sigma}^e+p_1\mathbf{I}):\mathbf{D}-\frac{\vec{q}\cdot\vec{\nabla}T}{T} &\geq 0\Rightarrow \\ -p_1\,\mathbf{D}:\mathbf{I}-\rho\left(\frac{\partial f}{\partial X}\right)\dot{X}+(\boldsymbol{\sigma}^e+p_1\mathbf{I}):\mathbf{D}-\frac{\vec{q}\cdot\vec{\nabla}T}{T} &\geq 0\Rightarrow \\ \boldsymbol{\sigma}^e:\mathbf{D}-\rho\left(\frac{\partial f}{\partial X}\right)\dot{X}-\frac{\vec{q}\cdot\vec{\nabla}T}{T} &\geq 0\end{aligned} \tag{A.13}$$

A.1.2 Elimination of $\dot{u}$ from the energybalance

Equations (A.9) showed that (ρ,T,X) sufficed as independent variables. Therefore the thermodynamic pressure depends upon these variables. In other words :
$p_0=p_0\,(\rho,T,X)$. Under the assumption that invertion is justified, we may write ;

$$\rho=\rho(p_0,T,X) \tag{A.14}$$

this leads to :

$$\dot{p}_0 = \left(\frac{\partial p_0}{\partial T}\right)_{\rho,X}\dot{T}+\left(\frac{\partial p_0}{\partial \rho}\right)_{T,X}\dot{\rho}+\left(\frac{\partial p_0}{\partial X}\right)_{T,\rho}\dot{X} \tag{A.15}$$

$$\dot{\rho} = \left(\frac{\partial \rho}{\partial T}\right)_{p_0,X}\dot{T}+\left(\frac{\partial \rho}{\partial p_0}\right)_{T,X}\dot{p}_0+\left(\frac{\partial \rho}{\partial X}\right)_{T,p_0}\dot{X} \tag{A.16}$$

Insertion of (A.15) in (A.16) gives ;

$$\dot{\rho}\left(1-\left(\frac{\partial\rho}{\partial p_0}\right)_{T,X}\left(\frac{\partial p_0}{\partial\rho}\right)_{T,X}\right)= \tag{A.17}$$
$$\left(\left(\frac{\partial\rho}{\partial p_0}\right)_{T,X}\left(\frac{\partial\rho}{\partial T}\right)_{\rho,X}+\left(\frac{\partial\rho}{\partial T}\right)_{p_0,X}\right)\dot{T}+\left(\left(\frac{\partial\rho}{\partial p_0}\right)_{T,X}\left(\frac{\partial p_0}{\partial X}\right)_{\rho,T}+\left(\frac{\partial\rho}{\partial X}\right)_{p_0,T}\right)\dot{X}$$

The left-hand-side is zero ánd $\dot{T}$, $\dot{X}$ can be chosen free so :

$$\begin{aligned}\left(\frac{\partial\rho}{\partial p_0}\right)_{T,X}\left(\frac{\partial p_0}{\partial T}\right)_{\rho,X}+\left(\frac{\partial\rho}{\partial T}\right)_{p_0,X} &= 0\\ \left(\frac{\partial\rho}{\partial p_0}\right)_{T,X}\left(\frac{\partial p_0}{\partial X}\right)_{\rho,T}+\left(\frac{\partial\rho}{\partial X}\right)_{p_0,X} &= 0\end{aligned} \tag{A.18}$$

The definition of the specific free energy, the definition of p_0, ánd Gibbs law, result in the following equations ;

$$\left.\begin{aligned}\left(\tfrac{\partial u}{\partial\rho}\right)_{T,X}=\tfrac{\partial}{\partial\rho}[f+Ts]_{T,X} &= \left(\tfrac{\partial f}{\partial\rho}\right)_{T,X}+T\left(\tfrac{\partial s}{\partial\rho}\right)_{T,X}\\ \left(\tfrac{\partial f}{\partial\rho}\right)_{T,X} &= 1/\rho^2\,p_0\\ \left(\tfrac{\partial s}{\partial\rho}\right)_{T,X} &= -1/\rho^2\left(\tfrac{\partial p_0}{\partial T}\right)_{\rho,X}\end{aligned}\right\}\Rightarrow$$

$$\left(\frac{\partial u}{\partial\rho}\right)_{T,X}=\frac{p_0}{\rho^2}-\frac{T}{\rho^2}\left(\frac{\partial p_0}{\partial T}\right)_{\rho,X} \tag{A.19}$$

Because $\dot{u}$ is a function of ρ, T, X, we may write ;

$$\dot{u}=\left[\frac{p_0}{\rho^2}-\frac{T}{\rho^2}\left(\frac{\partial p_0}{\partial T}\right)_{\rho,X}\right]\dot{\rho}+\left(\frac{\partial u}{\partial T}\right)_{\rho,X}\dot{T}+\left(\frac{\partial u}{\partial X}\right)_{\rho,T}\dot{X} \tag{A.20}$$

With the definition of heat capacity at constant specific volume $C_v=(\frac{\partial u}{\partial T})_{\rho,X}$ and $\rho=\rho(p_0,T,X)$ equation (A.20) becomes ;

$$\begin{aligned}\dot{u} &= \left[\frac{p_0}{\rho^2}-\frac{T}{\rho^2}\left(\frac{\partial p_0}{\partial T}\right)\right]\left[\left(\frac{\partial\rho}{\partial p_0}\right)\dot{p_0}+\left(\frac{\partial\rho}{\partial T}\right)\dot{T}+\left(\frac{\partial\rho}{\partial X}\right)\dot{X}\right]+C_v\dot{T}+\left(\frac{\partial u}{\partial X}\right)\dot{X}\Rightarrow\\ \dot{u} &= \left(\frac{p_0}{\rho^2}\left(\frac{\partial\rho}{\partial T}\right)-\frac{T}{\rho^2}\left(\frac{\partial p_0}{\partial T}\right)\left(\frac{\partial\rho}{\partial T}\right)\right)\dot{T}\\ &+ \left(\frac{p_0}{\rho^2}\left(\frac{\partial\rho}{\partial p_0}\right)-\frac{T}{\rho^2}\left(\frac{\partial p_0}{\partial T}\right)\left(\frac{\partial\rho}{\partial p_0}\right)\right)\dot{p_0}\\ &+ \left(\frac{p_0}{\rho^2}\left(\frac{\partial\rho}{\partial X}\right)-\frac{T}{\rho^2}\left(\frac{\partial p_0}{\partial T}\right)\left(\frac{\partial\rho}{\partial X}\right)\right)\dot{X}\\ &+ C_v\dot{T}+\left(\frac{\partial u}{\partial X}\right)\dot{X}\end{aligned} \tag{A.21}$$

With the identities (A.18) this becomes ;

$$\begin{aligned}
\dot{u} &= \left(\frac{p_0}{\rho^2}\left(\frac{\partial\rho}{\partial T}\right) + \frac{T}{\rho^2}\left(\frac{\partial p_0}{\partial T}\right)^2\left(\frac{\partial\rho}{\partial p_0}\right) + C_v\right)\dot{T} \\
&+ \left(\frac{p_0}{\rho^2}\left(\frac{\partial\rho}{\partial p_0}\right) + \frac{T}{\rho^2}\left(\frac{\partial\rho}{\partial T}\right)\right)\dot{p_0} \\
&+ \left(\frac{p_0}{\rho^2}\left(\frac{\partial\rho}{\partial X}\right) - \frac{T}{\rho^2}\left(\frac{\partial p_0}{\partial T}\right)\left(\frac{\partial\rho}{\partial X}\right) + \left(\frac{\partial u}{\partial X}\right)\right)\dot{X} \qquad \text{(A.22)}
\end{aligned}$$

more compact this can be written as ;

$$\begin{aligned}
\dot{u} &= \left(C_v - \frac{p_0}{\rho}\alpha + \frac{T}{\rho}\kappa\left(\frac{\partial p_0}{\partial T}\right)^2\right)\dot{T} \\
&+ \left(\frac{p_0}{\rho^2}\left(\frac{\partial\rho}{\partial p_0}\right) - \frac{T}{\rho^2}\left(\frac{\partial p_0}{\partial T}\right)\left(\frac{\partial\rho}{\partial p_0}\right)\right)\dot{p_0} \\
&+ \left(\frac{p_0}{\rho^2}\left(\frac{\partial\rho}{\partial X}\right) - \frac{T}{\rho^2}\left(\frac{\partial p_0}{\partial T}\right)\left(\frac{\partial\rho}{\partial X}\right) + \left(\frac{\partial u}{\partial X}\right)\right)\dot{X} \qquad \text{(A.23)}
\end{aligned}$$

where

$$\begin{aligned}
\alpha &= -\frac{1}{\rho}\left(\frac{\partial\rho}{\partial T}\right)_{p_0,X} \quad \text{volume expansion coëfficient} \\
\kappa &= \frac{1}{\rho}\left(\frac{\partial\rho}{\partial p_0}\right)_{T,X} \quad \text{isotherm compressibility factor} \\
\beta &= \frac{C_0}{\rho}\left(\frac{\partial\rho}{\partial X}\right)_{T,p_0} \quad \text{reaction shrinkage coëfficient}
\end{aligned}$$

Equation (A.23) has been deduced under the basic assumption of $u = u(\rho, T, X)$ where $\rho = \rho(p_0, T, X)$ has been taken into account.
This gives us u in terms of (p_0, T, X).

Instead of C_v we can also take C_p into account, briefly ;

$$u = u(p_0, T, X) \Rightarrow$$
$$\dot{u} = \left(\frac{\partial u}{\partial p_0}\right)_{T,X}\dot{p_0} + \left(\frac{\partial u}{\partial T}\right)_{p_0,X}\dot{T} + \left(\frac{\partial u}{\partial X}\right)_{p_0,T}\dot{X}$$

We introduce the specific enthalpy ;

$$h = u + \frac{p_0}{\rho} \Rightarrow$$
$$\left(\frac{\partial u}{\partial T}\right)_{p_0,X} = \frac{\partial}{\partial T}\left[h - \frac{p_0}{\rho}\right]_{p_0,X} = \left(\frac{\partial h}{\partial T}\right)_{p_0,X} - p_0\frac{\partial}{\partial T}\left(\frac{1}{\rho}\right)_{p_0,X}$$

$$= C_{p_0} - p_0 \frac{\partial}{\partial T}\left(\frac{1}{\rho}\right)_{p_0,X}$$
$$\Rightarrow$$

$$\dot{u} = \left(\frac{\partial u}{\partial p_0}\right)_{T,X} \dot{p_0} + \left[C_{p_0} + \frac{p_0}{\rho^2}\left(\frac{\partial \rho}{\partial T}\right)_{p_0,X}\right] \dot{T} + \left(\frac{\partial u}{\partial X}\right)_{p_0,X} \dot{X} \qquad \text{(A.24)}$$

with

$$\left(\frac{\partial u}{\partial X}\right)_{p_0,T} = \frac{\partial}{\partial X}\left[h - \frac{p_0}{\rho}\right]_{p_0,T} = \left(\frac{\partial h}{\partial X}\right)_{p_0,T} - p_0 \frac{\partial}{\partial X}\left(\frac{1}{\rho}\right)_{p_0,T}$$
$$= h_r + \frac{p_0}{\rho^2}\left(\frac{\partial \rho}{\partial X}\right)_{p_0,T}$$

this becomes ;

$$\dot{u} = \left(\frac{\partial u}{\partial p_0}\right)_{T,X} \dot{p_0} + \left[C_{p_0} + \frac{p_0}{\rho^2}\left(\frac{\partial \rho}{\partial T}\right)_{p_0,X}\right] \dot{T} + \left[h_r + \frac{p_0}{\rho^2}\left(\frac{\partial \rho}{\partial X}\right)_{p_0,T}\right] \dot{X} \qquad \text{(A.25)}$$

equation (A.23) shows ;

$$\left(\frac{\partial u}{\partial p_0}\right)_{T,X} = \left(\frac{p_0}{\rho^2}\left(\frac{\partial \rho}{\partial p_0}\right)_{T,X} - \frac{T}{\rho^2}\left(\frac{\partial p_0}{\partial T}\right)\left(\frac{\partial \rho}{\partial p_0}\right)\right)$$
$$= \frac{p_0}{\rho^2}\left(\frac{\partial \rho}{\partial p_0}\right)_{T,X} + \frac{T}{\rho^2}\left(\frac{\partial \rho}{\partial T}\right)_{p_0,X} \quad \text{(see (A.18))}$$
$$= \frac{p_0}{\rho^2}\left(\frac{\partial \rho}{\partial p_0}\right)_{T,X} - \frac{T}{\rho}\alpha \qquad \text{(A.26)}$$

(A.27)

Insertion of this equality in (A.26) gives the following expression ;

$$\dot{u} = \left[\frac{p_0}{\rho^2}\left(\frac{\partial \rho}{\partial p_0}\right)_{T,X} - \frac{T}{\rho}\alpha\right] \dot{p_0} + \left[C_{p_0} + \frac{p_0}{\rho^2}\left(\frac{\partial \rho}{\partial T}\right)_{p_0,X}\right] \dot{T} + \left[h_r + \frac{p_0}{\rho^2}\left(\frac{\partial \rho}{\partial X}\right)_{p_0,T}\right] \dot{X}$$
$$= -\frac{T}{\rho}\alpha \dot{p_0} + C_{p_0}\dot{T} + h_r \dot{X} + \frac{p_0}{\rho^2}\left[\frac{\partial \rho}{\partial p_0}\dot{p_0} + \frac{\partial \rho}{\partial T}\dot{T} + \frac{\partial \rho}{\partial X}\dot{X}\right]$$
$$= -\frac{T}{\rho}\alpha \dot{p_0} + C_{p_0}\dot{T} + h_r \dot{X} + \underbrace{\frac{p_0}{\rho^2}\dot{\rho}}_{\downarrow}$$

$$\frac{p_0}{\rho}\frac{\dot{\rho}}{\rho} = \frac{p_0}{\rho}\left(-\frac{\dot{J}}{J}\right) = -\frac{p_0}{\rho} tr(\mathbf{D}) \qquad \text{(A.28)}$$

therefore ;

$$\dot{u} = -\frac{T}{\rho}\alpha\dot{p_0} + C_{p_0}\dot{T} + h_r\dot{X} - \frac{p_0}{\rho}tr(\mathbf{D}) \tag{A.29}$$

Using this expression to eliminate $\dot{u}$ from the energy balance,

$$\rho\dot{u} = -\vec{\nabla}\cdot\vec{q} + \boldsymbol{\sigma} : \mathbf{D} + \rho r_r \tag{A.30}$$

gives;

$$\rho C_{p_0}\dot{T} = -\vec{\nabla}\cdot\vec{q} + T\alpha\dot{p_0} + \underbrace{\underbrace{p_0\, tr(\mathbf{D}) + \boldsymbol{\sigma} : \mathbf{D}}_{p_0\mathbf{I} : \mathbf{D} + \boldsymbol{\sigma} : \mathbf{D}}}_{p_0\mathbf{I} : \mathbf{D} + (-p_0\mathbf{I} + \boldsymbol{\sigma}^e) : \mathbf{D}} + \rho\, r_r - \rho\, h_r\dot{X}$$

$$\boldsymbol{\sigma}^e : \mathbf{D}$$

with $\rho\, h_r = H_r$ and the mole balance, neglecting diffusion ;

$$\frac{dC}{dt} = -C_0\frac{dX}{dt} = -R \tag{A.31}$$

the energy balance can be written as :

$$\rho C_{p_0}\dot{T} = -\vec{\nabla}\cdot\vec{q} + T\alpha\dot{p_0} + \boldsymbol{\sigma}^e : \mathbf{D} + \rho\, r_r - \frac{H_r}{C_0}R \tag{A.32}$$

A.1.3 dimensionless groups

A dimensionless group is any combination of dimensional or dimensionless quantities possessing zero overall dimensions [8] The introduction of dimensionless groups and the resulting dimensionless numbers, reduces the number of variables. It also makes a balance equation independent of the scale and therefore comparable to modelsituations (if the dimensionless numbers are of the same size). Next to this it is possible to give an order of magnitude estimate of the various terms in a balance.

The choise of the scale factors depends on the problem one wishes to describe; the scale factors have to be characteristic for the specific problem. In general this doesn't present any difficulties, it is for example obvious to scale concentration at the start-of-process concentration. To scale the temperature however, several possibilities arise. For the time being, this choise is postponed. We introduce the following characteristic values :

$$
\begin{array}{llllll}
T^* & = & \frac{T-T_0}{\Delta T} & & & \text{(choise for } \Delta T \text{ will be discussed furtheron)} \\
p_0^* & = & p_0(\frac{r_0}{\eta_0 V}) & & & \text{(with respect to shear stress)} \\
v^* & = & \frac{v}{V} & \epsilon & = & \frac{r_0}{L} \\
\alpha^* & = & \frac{\alpha}{\alpha_0} & \lambda^* & = & \frac{\lambda}{\lambda_0} \\
\eta^* & = & \frac{\eta}{\eta_0} & \kappa^* & = & \frac{\kappa}{\kappa_0} \\
\beta^* & = & \frac{\beta}{\beta_0} & \rho^* & = & \frac{\rho}{\rho_0} \\
C_{p_0}^* & = & \frac{C_{p_0}}{C'_{p_0}} & t^* & = & \frac{tV}{L} = \frac{t}{t_0} \\
R^* & = & \frac{R}{C_0} t_r & \vec{\nabla}^* & = & \vec{\nabla} r_0 \\
C^* & = & \frac{C}{C_0} & \vec{g}^* & = & \frac{\vec{g}}{g}
\end{array}
$$

In the case of channel flow r_0 denotes the dimension measured perpendicular to the flowlines and L is a larger scale measured along the flow lines. Define the shear rate :

$$
\begin{aligned}
\sqrt{II} &= \sqrt{\frac{1}{2}(\vec{\nabla}\vec{v} + (\vec{\nabla}\vec{v})^c) : (\vec{\nabla}\vec{v} + (\vec{\nabla}\vec{v})^c)} \\
&= \sqrt{2\mathbf{D} : \mathbf{D}}
\end{aligned} \tag{A.33}
$$

Aplying Fourier's law, $\vec{q} = -\lambda\vec{\nabla}T$ and not considering radiation, the energy balance becomes :

$$
\begin{aligned}
&\frac{\rho_0 C'_{p_0} \Delta T \epsilon V}{r_0} \rho^* C_{p_0}^* \dot{T}^* = \\
&\quad \frac{\Delta T \lambda_0}{r_0^2}(\vec{\nabla} \cdot \lambda\vec{\nabla}T) + \frac{\alpha_0 \eta_0 V^2 \epsilon}{r_0^2}(T_0 + \Delta T T^*)\alpha^* \dot{p_0}^* \\
&\quad + \frac{\eta_0 V^2}{r_0^2}\eta^* II^* - \frac{H_r}{t_r} R^*
\end{aligned}
$$

$\Rightarrow$

$$
\begin{aligned}
&\frac{\rho_0 r_0 C'_{p_0} \epsilon V}{\lambda_0} \rho^* C_{p_0}^* \dot{T}^* = \\
&\quad (\vec{\nabla} \cdot \lambda\vec{\nabla}T) \\
&\quad + \frac{\alpha_0 \eta_0 V^2 \epsilon}{\lambda_0}(\frac{T_0}{\Delta T} + T^*)\alpha^* \dot{p_0}^* \\
&\quad + \frac{\eta_0 V^2}{\Delta T \lambda_0}\eta^* II^* - \frac{r_0^2 \rho_0 h_r}{\Delta T \lambda_0 t_r}\rho^* R^*
\end{aligned} \tag{A.34}
$$

The first dimensionless group that appears is ;

$$
\frac{\rho_0 r_0 C'_{p_0} \epsilon V}{\lambda_0} = \frac{\rho_0 r_0^2 C'_{p_0}}{\lambda_0 t_0} = Gz \tag{A.35}
$$

(A.35) is the Graetz number. It presents the ratio of heat convection along the stream and heat conduction across the stream.
The interpretation of the other dimensionless groups depends on the ΔT that is used. The following choises can be considered ;

- $\Delta T = \Delta T_{op} = \mid T_w - T_0 \mid$
  T_w is the wall temperature and T_0 is the initial melt temperature. This scale factor is used quite often. The accompanying dimensionless numbers are :

$$\frac{\eta_0 V^2}{\Delta T_{op} \lambda_0} = Br \tag{A.36}$$

Equation (A.36) represents the socalled Brinkman number, it reflects the ratio of heat produced by viscous dissipation and by heat conduction with respect to the viscosity. In other words, will the heat production by dissipation or the imposed wall temperature give an effective change in the melt viscosity.

$$\frac{r_0^2 \rho_0 h_r}{\Delta T_{op} \lambda_0 t_r} = DaIV \tag{A.37}$$

Equation (A.37) is the DamköhlerIV number; the ratio of chemical produced heat and heat conduction. Following [6], t_r represents the isothermal cure time, given by :

$$t_r = \int_{X=0}^{X_{end}} \frac{C_0}{R|_{T_w}} dX \tag{A.38}$$

here C_0 is the initial concentration of reactive species, X is the extent of reaction and R is the reaction rate for constant temperature $T = T_w$.

$$\frac{\alpha_0 \eta_0 V^2 \epsilon}{\lambda_0} = \epsilon \frac{Br}{Ga} \tag{A.39}$$

where $Ga = \frac{1}{\alpha_0 \Delta T}$ (a measure for temparature causing a change of volume), equation (A.39) represents the Gay-Lussac number. This number is a ratio of heat produced by pressure change and heat conduction.

- $\Delta T = \Delta T_{rheol} = \mid \eta / \frac{\partial \eta}{\partial T} \mid$

The magnitude of this scale factor is an indication if large viscosity changes are to be expected as a result of temperature changes.

In the case of large ΔT_{rheol} the coupling of energy- and momentum balance by viscosity can be cancelled. The viscosity can be considered independant of temperature.

$$\frac{\eta_0 V^2}{\Delta T_{rheol} \lambda_0} = G \tag{A.40}$$

Equation (A.40) is the Nahme Griffith number; The magnitude of this number determines wether heat production by dissipation will cause a substantial change of viscosity, a change large enough to influence the velocity field.

$$\frac{r_0^2 \rho_0 h_r}{\triangle T_{rheol} \lambda_0 t_r} \tag{A.41}$$

Number (A.41) has the same meaning as (A.40) with respect to chemical reaction. In the case of not fully developed flow in a channel, the Nahme Griffith number can be evaluated at T_0 :

$$G_0 = \frac{\eta_0 V^2}{\lambda_0 (\triangle T_{rheol})_0} \tag{A.42}$$

- $G_0/Gz \ll 1$
  Heat production by dissipation can be ignored.
- $G_0/Gz = 1$
  Heat production by dissipation can not be ignored.
- $G_0 \gg 1$
  Heat production by dissipation is dominant.

- $\triangle T = \triangle T_{ad} = \frac{p_0'}{\rho_0 C_{p_0}'}$

According to [9] this scale is based on full conversion of work into heat.

$$\frac{\eta_0 V^2}{\triangle T_{ad} \lambda_0} = Pe \tag{A.43}$$

Equation (A.43) is the Peclet number; the ratio of heat convection along the stream and heat conduction along the stream. p_0' is i.e. a characteristic pressure we related to the shear stress;

$$\begin{aligned} p_0' &= \frac{\eta_0 V}{r_0} \Rightarrow \\ \frac{\eta_0 V^2}{\triangle T_{ad} \lambda_0} &= \frac{\eta_0 V^2 \rho_0 C_{p_0}' r_0}{\eta_0 V \lambda_0} = \frac{\rho_0 C_{p_0}' V r_0}{\lambda_0} \end{aligned}$$

- $\triangle T = \triangle T_{gen} = \frac{\eta_0 V^2}{\lambda_0}$

According to [9] this factor presents a balance between heat production and heat conduction. Both terms are in fact considered to be of the same size; in the energy balance, the dimensionless conduction and dissipation groups are scaled to 1;

$$\frac{\eta_0 V^2}{\triangle T_{gen} \lambda_0} = 1 \tag{A.44}$$

- $\Delta T = \Delta T_{chem} = T_{crit} - T_w$
  T_{crit} is the temparature the melt starts to show thermal degradation at. This temperature scale is especially of interest to the "process-boys". I will pay no further attention to it here.

According to [9], ΔT_{op} is a useful scale factor if $\Delta T_{op} \ll \Delta T_{rheol}$, if this is not the case, the Graetz number has to be determined to make the right choise. If $\Delta T_{op} \ll \Delta T_{rheol}$, the imposed temperature difference will not result in a considerable viscosity change. Therefore if ΔT_{op} is not extremely small compared to other temperature differences that will arise, ΔT_{op} provides a suitable temperature case and ΔT_{rheol} will not be significant for the process.

If $Gz \ll 1$, the process is said to be stationary, convection is negligible. This may be illustrated by tube flow when the flow will be fully developed over most of the tube length. The initial temperature, T_0 , is no longer of importance to the process ; and therefore the scale ΔT_{op} is no longer relevant. Because conduction can not be ignored, ΔT_{ad} becomes irrelevant. ΔT_{rheol} is the most sensible choice.

If $Gz = 1$, $\Delta T_{op}, \Delta T_{gen}$ and ΔT_{ad} can all be relevant

If $Gz \gg 1$, conduction is dominated by convection.

In view of reactive flow that occurs during polymer processing (especially IC-packaging) and the case that is simulated (piston driven and driving flow), the following values are of interest ;

$$
\begin{array}{llll}
T_0 & = & 293[K] & \\
T_w & = & 393[K] & \\
(\frac{\partial \eta}{\partial T}) & = & 10^5[\frac{Pa\,s}{^0C}] & \\
\eta_0 & = & 10^5[Pa\,s] \text{ at } T = 393[K] \text{ and} \sqrt{II_0} = \frac{V}{r_0} = 1 & \\
\kappa_0 & = & 10^{-9}[\frac{m^2}{N}] & D = 10^{-13}[\frac{m^2}{S}] \\
\alpha_0 & = & 10^{-9}[\frac{1}{^0C}] & V = 10^{-3}[\frac{m}{s^2}] \\
p_0' & = & 10^4[\frac{N}{m^2}] & \lambda_0 = 10^{-1}[\frac{J}{mKs}] \\
\rho_0 & = & 10^3[\frac{kg}{m^3}] & C_{p_0}' = 10^3[\frac{J}{kg^0C}] \\
h_r & = & -10^4[\frac{J}{kg}] & \epsilon = 10^{-1} \\
r_0 & = & 10^{-2}[m] & t_r = 10^3[s] \text{ at } T = 393[K]
\end{array}
$$

This in the following temperature scales and dimensionless numbers;

$$
\begin{aligned}
\Delta T_{op} &= 10^2 \\
\Delta T_{rheol} &= 1 \\
\Delta T_{ad} &= 10^4 \\
\Delta T_{gen} &= 10^1
\end{aligned}
$$

$$
\begin{aligned}
Gz &= 10^2 \\
G_0 &= 10^1 \\
Br &= 10^{-2} \\
Ga &= 10^7
\end{aligned}
$$

The Nahme Griffith indicates there is sufficient dissipation to influence the viscosity. The Brinkman number shows that the imposed temperature difference are considerable larger than the temperature rise due to viscous dissipation. As convection obviously playes an important role, ΔT_{op} is the appropriate scale factor. This gives the following order of magnitude estimation ;

internal energy	:	$O(10)$
conduction	:	$O(1)$
pressure	:	$O(10^{-12})$
dissipation	:	$O(10^{-2})$
reaction	:	$O(10^{-1})$

On account of the above the pressure term can be neglected in the energy balance. Consequently the energy balance reduces to ;

$$
\begin{aligned}
&\rho^* C^*_{p_0} Gz \dot{T}^* = \\
&\quad (\vec{\nabla} \cdot \lambda \vec{\nabla} T) + Br\eta^* II - DaIV\rho^* R^*
\end{aligned} \tag{A.45}
$$

A.2 The mole balance

Consider a system consisting of n components amongst which r chemical reactions are possible. If S_j $[\frac{mol}{m^3 s}]$ is the chemical reaction rate for the j^{th} reaction, the production of component k equals :

$$
M_{wk} m_{kj} S_j \, [\frac{kg}{m^3 s}] \tag{A.46}
$$

in which M_{wk} is the mole mass of component k and m_{kj} is the stochiometric coëfficient of component k in the j^{th} reaction, counted positive when appearing in the second member, negative when appearing in the first member of the reaction equation.

For a volume $V(t)$ the total production of k due to chemical reactions which occur inside $V(t)$, becomes :

$$
\sum_{j=1}^{r} \int_{V(t)} M_{wk} m_{kj} S_j \, dv \tag{A.47}
$$

Because of conservation of mass, the rate of change of mass of component k within volume $V(t)$ is :

$$\frac{d}{dt}\int_{V(t)} -\rho_k \, dv = \sum_{j=1}^{r} \int_{V(t)} M_{wk} m_{kj} S_j \, dv \tag{A.48}$$

Appplying Gauss' theorem to the integral occuring in (A.48) we obtain :

$$\frac{\partial \rho_k}{\partial t} + \vec{\nabla} \cdot (\vec{v}_k \rho_k) = \sum_{j=1}^{r} M_{wk} m_{kj} S_j \tag{A.49}$$

in which $\vec{v}_k$ is the velocity of component k.
Summing equation (A.49) over all components k gives the equation of mass :

$$\frac{\partial \rho}{\partial t} + \vec{\nabla} \cdot (\rho \vec{v}) = 0 \tag{A.50}$$

The substantial time derivative of ρ_k is :

$$\frac{d\rho_k}{dt} = \frac{\partial \rho_k}{\partial t} + \vec{v} \cdot \vec{\nabla} \rho_k \tag{A.51}$$

where $\vec{v}$ is the centre of mass velocity :

$$\vec{v} = \sum_{k=1}^{n} \frac{\rho_k \vec{v}_k}{\rho} \tag{A.52}$$

In a diffusing mixture the various chemical components are moving at different velocities $\vec{v}_k$. For a mixture of n components the local mass average velocity is $\vec{v}$.
With equation (A.49), (A.51) can be written as :

$$\begin{aligned} \frac{d\rho_k}{dt} &= -\vec{\nabla} \cdot (\vec{v}_k \rho_k) + \sum_{j=1}^{r} M_{wk} m_{kj} S_j + \vec{v} \cdot \vec{\nabla} \rho_k \\ &= -\vec{\nabla} \cdot \rho_k (\vec{v}_k - \vec{v}) - \rho_k \vec{\nabla} \cdot \vec{v} + \sum_{j=1}^{r} M_{wk} m_{kj} S_j \end{aligned} \tag{A.53}$$

$(\vec{v}_k - \vec{v})$ is a velocity indicating motion of component k relative to the local motion of the stream.
If molar concentration C_k :

$$C_k = \frac{\rho_k}{M_{wk}} \left[\frac{mol}{m^3}\right] \tag{A.54}$$

is employed, equation (A.53) reduces to :

$$\frac{dC_k}{dt} + C_k\vec{\nabla}\cdot\vec{v} = -\vec{\nabla}\cdot\vec{J} + \sum_{j=1}^{r} m_{kj}S_j \tag{A.55}$$

in which $\vec{J}\,[\frac{mol}{m^2 s}]$ is the molar flux. As a constitutive equation for the molar flux a function of the concentration gradient is chosen :

$$\vec{J} = -\mathcal{D}\cdot\vec{\nabla}C_k \tag{A.56}$$

where $\mathcal{D}$ is the diffusion tensor. If $\mathcal{D}$ is considered constant, for an isotropic material (A.56) becomes :

$$\vec{J} = -D\vec{\nabla}C_k \tag{A.57}$$

Insertion of (A.57) into equation (A.55) this can be written as :

$$\frac{dC_k}{dt} + C_k\vec{\nabla}\cdot\vec{v} = D\vec{\nabla}^2 C_k + \sum_{j=1}^{r} m_{kj}S_j \tag{A.58}$$

or

$$\frac{\partial C_k}{\partial t} + \vec{\nabla}\cdot(\vec{v}C_k) = D\vec{\nabla}^2 C_k + \sum_{j=1}^{r} m_{kj}S_j \tag{A.59}$$

For incompressible fluids this reduces to :

$$\frac{dC_k}{dt} = D\vec{\nabla}^2 C_k + \sum_{j=1}^{r} m_{kj}S_j \tag{A.60}$$

The reaction term in this equation is not easy to determine. It depends on temperature and concentration of the components. Often phenomenologic relations are used, that do not represent the real mechanism of the reaction during the whole process, but are adequate to describe the overall chemical reaction for certain systems.
We then write :

$$\frac{dC_k}{dt} = D\vec{\nabla}^2 C_k - R(T, C_k) \tag{A.61}$$

where R is the rate of polymer production, which is opposite to the production of component k. Considering binary systems this reduces the balance equation to the following :

$$\frac{dC}{dt} = D\vec{\nabla}^2 C - R \tag{A.62}$$

Equation (A.62) can be made dimensionless by the introduction of characteristic values :

$$\frac{dC^*}{dt^*} = \frac{D}{Vr_0}(\vec{\nabla}^{*2}C^*) - \frac{r_0}{Vt_r}R^* \tag{A.63}$$

The reaction term is accompanied by :

$$\frac{r_0}{Vt_r} = \frac{t_0}{t_r} = DaI \tag{A.64}$$

DaI, the Dämkohler I number gives the reaction rate to flow rate ratio. In our case :

$$DaI = 0.02 \tag{A.65}$$

if the characteristic reaction time t_r is defined as the isothermal cure time at the wall for $T = T_w = 393[K]$.
In the case of reacting monomers we can often neglect molecular diffusion because of very large mass transfer Peclet numbers ([2]) :

$$\frac{r_0 V}{D} = Pe_m \tag{A.66}$$

in our case :

$$\frac{1}{Pe_m} = 10^{-8} \tag{A.67}$$

Neglecting molecular diffusion, the dimensionless mole balance becomes :

$$\frac{dC^*}{dt^*} = -DaIR^* \tag{A.68}$$

Instead of concentration C, the extent of reaction X is often used :

$$X = \frac{C_0 - C}{C_0} \tag{A.69}$$

also known as conversion. C_0 is the initial concentration of reactive species.

A.3 The continuity equation

For reacting materials :

$$\dot{\rho} = -\rho(\vec{\nabla} \cdot \vec{v}) = \left(\frac{\partial \rho}{\partial T}\right)_{p_0,X} \dot{T} + \left(\frac{\partial \rho}{\partial p_0}\right)_{T,X} \dot{p_0} + \left(\frac{\partial \rho}{\partial X}\right)_{T,p_0} \dot{X} \tag{A.70}$$

using the definitions of α, κ, β this becomes :

$$-(\vec{\nabla} \cdot \vec{v}) = -\alpha \dot{T} + \kappa \dot{p_0} + \frac{\beta}{C_0} \dot{X} \tag{A.71}$$

Introducing the characteristic values :

$$(\vec{\nabla}^* \cdot \vec{v}^*) = \alpha_0 (T_1 - T_0) \alpha^* \dot{T}^* + \frac{\kappa_0 \eta_0 V}{r_0} \dot{p_0}^* \kappa - \frac{\beta_0}{C_0} \beta^* \dot{X} \tag{A.72}$$

Notice that $X = X^*$, the conversion is already dimensionless. The "scale factor" that has been used is that of conversion of fully cured material ; $C = 0, X_0 = 1$.
the dimensionless numbers that can be distinguished are :

$$\frac{1}{\alpha_0 (T_1 - T_0)} = Ga \tag{A.73}$$

Ga is the Gay Lussac number. Its reciprocal value reflects change of volume by temperature change.

$$\rho_0 V^2 \kappa_0 = Ca \tag{A.74}$$

Ca is the Cauchy number, it is the ratio of inertia forces to elastic forces.

$$\frac{\rho_0 V r_0}{\eta_0} = Re \tag{A.75}$$

Re is the well known Reynolds. The balance of mass can therefore be written as :

$$(\vec{\nabla}^* \cdot \vec{v}^*) = \frac{1}{Ga} \alpha^* \dot{T}^* - \frac{Ca}{Re} \kappa^* \dot{p_0}^* - \frac{\beta_0}{C_0} \beta^* \dot{X} \tag{A.76}$$

The order of magnitude of the various terms in the balance can be estimated :

volume change by temperature change : $O(10^{-7})$
volume change by pressure change : $O(10^{-6})$

If the shrinkage of the polymer is small then the volume change by chemical reaction can be neglected. Consequently the mass balance reads :

$$(\vec{\nabla} \cdot \vec{v}) = 0 \tag{A.77}$$

A.4 The momentum balance

In general :

$$\rho \dot{\vec{v}} = \vec{\nabla} \cdot \boldsymbol{\sigma} + \rho \vec{g} \tag{A.78}$$

For the materials involved, generalized Newtonian behaviour is assumed. When the bulkviscosity is considered to be zero $\mu = 0$, the stress tensor becomes :

$$\begin{aligned} \boldsymbol{\sigma} = -p_0\mathbf{I} + \boldsymbol{\sigma}^e &= -p_0\mathbf{I} + \mu tr(\mathbf{D})\mathbf{I} + \boldsymbol{\sigma}^d \\ &= -p_0\mathbf{I} + 2\eta\mathbf{D}^d \end{aligned} \tag{A.79}$$

where p_0 is the thermodynamic pressure, $\mathbf{D}$ is the rate of strain tensor and $\boldsymbol{\sigma}^e$ is called the extra stress tensor. Then :

$$\rho\dot{\vec{v}} = \vec{\nabla}\cdot\boldsymbol{\sigma}^d - \vec{\nabla}p_0 + \rho\vec{g} \tag{A.80}$$

Equation (A.80) can be made dimensionless, this gives :

$$\frac{\rho_0 V r_0}{\eta_0}\rho^*\dot{\vec{v}}^* = 2\vec{\nabla}^*\cdot\eta^*\mathbf{D}^{d^*} - \vec{\nabla}^*p^* + \frac{\rho_0 r_0^2 g}{\eta_0 V}\rho^* g^* \tag{A.81}$$

In equation (A.81) the following dimensionless numbers can be recognized :

$$\frac{\rho_0 V r_0}{\eta_0} = Re \tag{A.82}$$

(A.82) is the Reynolds number; the ratio of inertia forces to viscous forces.

$$\frac{V^2}{g r_0} = Fr \tag{A.83}$$

(A.83) is the Froude number; the ratio of inertia forces to gravity forces. Introduction of (A.82) and (A.83) into (A.81) gives :

$$Re\ \rho^*\dot{\vec{v}}^* = 2\vec{\nabla}^*\cdot\eta^*\mathbf{D}^{d^*} - \vec{\nabla}^*p^* + \frac{Re}{Fr}\rho^* g^* \tag{A.84}$$

The magnitude of the dimensionless groups, reflects the importance of the accompanying mechanism. Estimation of these groups gives :

$$Re = 10^{-6} \tag{A.85}$$

$$Fr = 10^{-5} \tag{A.86}$$

It is reasonable to neglect the gravitational forces and inertia forces, because they are very small compared to pressure- and viscous force.

Appendix B

Results

In the simulations of piston driven and driving flow, the solution of the conversion equation shows oscillations in the region near the cornerpoints. This behaviour can be suppressed by upwinding techniques. These methods are based on adding an artificial diffusion to the convection-diffusion equation [3]. A disadvantage of this approach is the innacuracy in the solution due to the upwinding. However in a physical sense, fidelity is gained. In the case of a single heated wall, the error made can be limited by restricting the introduced diffusion to one direction. If this direction doesn't show a steep solution gradient, the error will be small.
To investigate the influence of artificial diffusion, a study has been made where the artificial diffusion is added in linear direction of the cavity. Because the conversion doesn't vary a great deal in this direction, this can be justified. Near the pistons however, it would be better to rotate the direction of diffusion 90^0 because the conversion is transported in cross direction and so is its gradient. However, because of the no-slip condition, material with high extent of reaction will stick to the wall and the conversion field in the piston regions will be smoother than near the heated wall. Therefore the influence of the diffusion in these regions is supposed to be small.

Fig. (B.1) shows the conversion fields for various diffusion coefficients with a wall temperature of $T_W = 384[K]$ at $t = 308[s]$. The diffusion coefficients in linear direction are $d_{22} = 10^{-6}$, 10^{-7} and $10^{-8}[\frac{m^2}{s}]$. The diffusion coefficients in cross direction are $d_{11} = 0[\frac{m^2}{s}]$. The extent of reaction at the wall can be calculated by integration of the reaction rate. At $t = 308[s]$ this conversion is $X_w = 0.133[-]$. Halfway the cavity length this value is maintained in all three cases and is not influenced by the artificial diffusion. In the two higher diffusion coefficient cases this maximum conversion level is not exceeded by numerical oscillations. In the lower diffusion coefficient case however, interpretation of the contour levels is hindered by the amplitude of the oscillations. Next to the driven piston region they also appear at the driving piston. Due to the multitude and level of the wiggles, the complete area is affected by these disturbances. For the cases where $d_{22} > 10^{-8}$ it can be noted that the oscillations only appear near the driven piston. The increased diffusion is capable of suppresssing the oscillations in the upper region. Because conversion increases from zero to unity, it can be expected that the oscillations produce negative conversion values. The level of this negative conversion decreases for increasing diffusion. As mentioned before, the diffusion should be pointed

parallel to the contour levels to minimize the introduced error. This is not the case near the pistons and as may be seen , the diffusion causes the contour levels to adopt a less sharp shape. In general : the higher the diffusion , the smoother the contour levels. Comparing the two higher diffusion coefficient cases shows that increasing the diffusion with a factor 10, causes a difference of 0.01 in extent of reaction near the driving piston. The region halfway the cavity length remains practically unchanged.
Next to the diffusion in linear direction, some simulations were carried out where diffusion is permitted in two directions.

As may be seen from fig. (B.2) this influence is very large. Fig. (B.2) shows contour levels of conversion and a conversion profile with $T_w = 384[K]$ and $d_{11} = d_{22} = 10^{-7}[\frac{m^2}{s}]$ at $t = 308[s]$. The conversion profile is taken halfway the cavity length. Note that the conversion at the wall is a factor 4.5 too small. The conversion near the cavity centre is a factor 2.5 larger than the similar case with no diffusion in cross direction. Evidently the difusion damps the conversion over the whole area. The conversion peak at the wall and the steep gradient are smoothend. In fact the conversion profile no longer represents a physical realistic image. As shown before, the conversion gradient at the wall will be very steep if no diffusion in cross direction is allowed. Fig. (B.2) shows a wall conversion gradient that approaches zero. The contour plot is practically oscillation free and negative conversion values do not occur.

Fig. (B.3) shows the viscosity distribution at $t = 308[s]$ for a wall temperature of $T_w = 393[K]$. In this case streamline upwinding has been used. The viscosity shows a rather irregular course. Near the cornerpoints a steep viscosity gradient in cross direction can be seen. Along the rest of the heated wall, this gradient is smaller. This is partly due to the mesh that is refined near the corners but that is coarser along the rest of the solid wall. Another reason for the irregularities is the way the viscosity is determined. The viscosity is computed as a function of shear rate, temperature and conversion. When this conversion reaches the gelpoint, an epoxy compound will behave like a solid [5]. This means that the viscosity becomes infinit. In the simulations this behaviour is modelled by increasing the viscosity to a finit value. In fact the viscosity is set to $10^7[Pas]$. The conversion gradient can be very steep and therefore the viscosity change can also be quite drastically. This can be a problem for the determination of the viscosity in the centroid of the extended quadratic elements that have been used to compute the velocities. To avoid this problem a linear interpolation of the viscosity from vertices to nodal points is performed. See appendix D. As can be seen from fig. (B.3) the viscosity reaches $10^7[Pas]$ at the wall. The conversion is beyond gelpoint only over a small distance from the heated wall. This results in a thin layer of high-viscosity material near the wall. After a small distance the viscosity drops considerably. Near the cornerpoints the element size is small enough to reproduce this drop. Along the rest of the wall the thickness of the gellayer doesn't cover an elementlength and therefore the lineair interpolation causes an overall viscosity level that is higher than at the cornerpoints. Refinement of the mesh can provide a more reliable viscosity field. The high level of viscosity that occurs at the driving piston is the result of material that has been transported from the wall to the piston. Closer to the midplane the high viscosity is caused by oscillations.

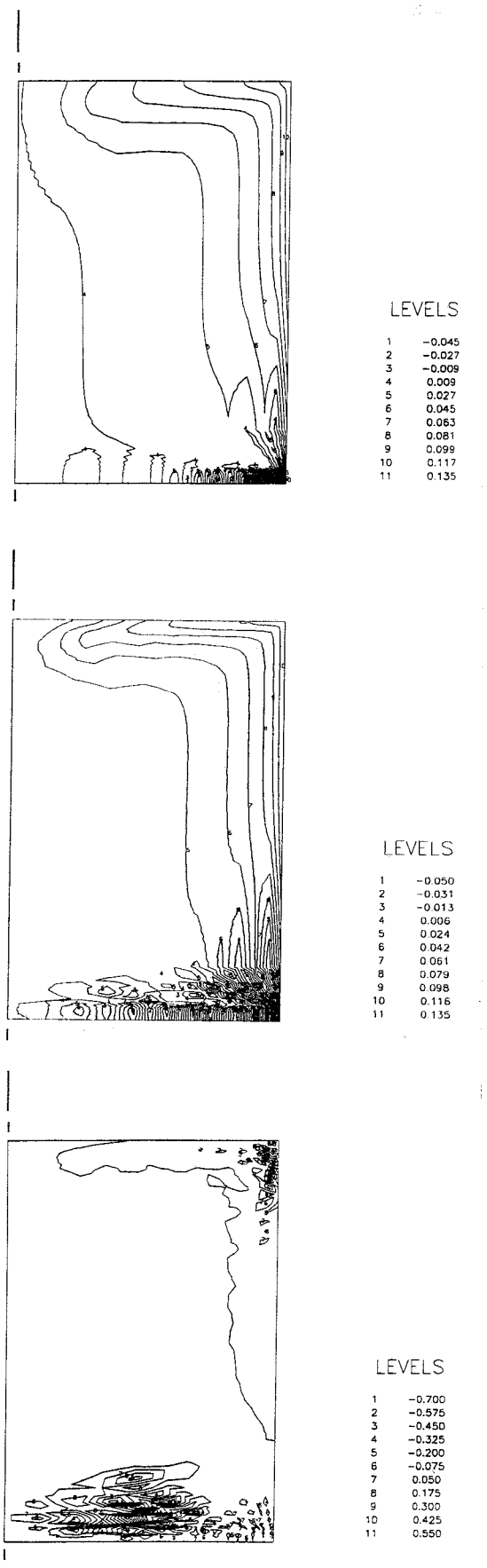

Figure B.1: Contour levels of conversion for different diffusion coefficients in linear direction.
$d_{11} = 0, d_{22} = 10^{-6}, 10^{-7}$ and $10^{-8}[\frac{m^2}{s}]$.
$T_w = 384[K], t = 308[s]$.

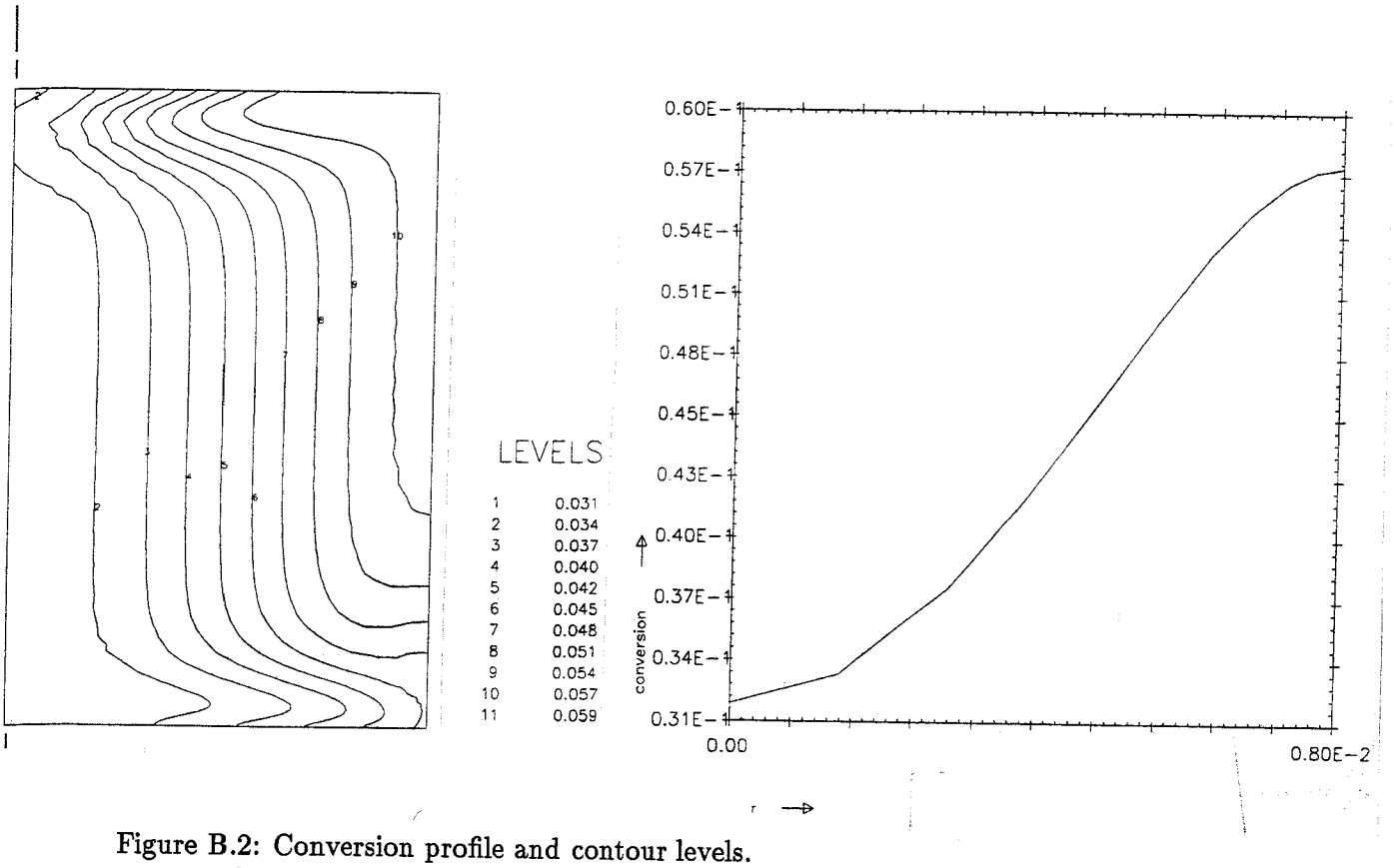

Figure B.2: Conversion profile and contour levels.
$T_w = 393[K], t = 308[s], d_{11} = d_{22} = 10^{-7}$.

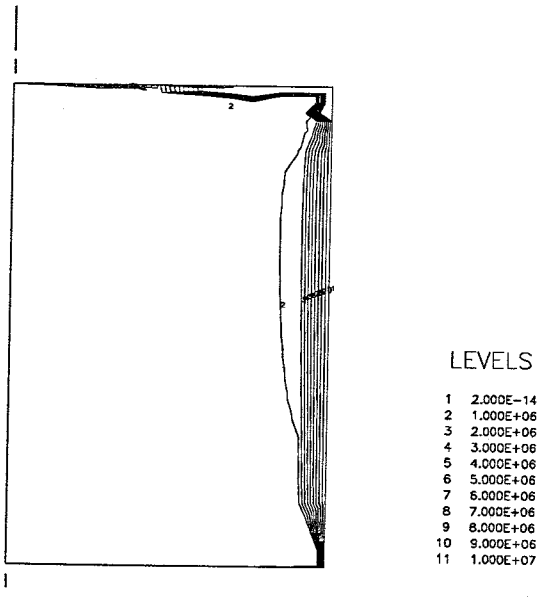

Figure B.3: Contour levels of viscosity.$T_w = 393[K], t = 308[s]$.

Appendix C

Rheology and kinetics

In order to simulate reactive flow, constitutive relations have to be used to describe chemical kinetics and the dynamic viscosity. For an epoxy compound these relations are proposed by Spoelstra et.al. [11]. The kinetics are determined by differential scanning calorimetry. The viscosity is described as a function of temperature, conversion and shear rate. Following Kamal and Sourour [7], the reaction rate of conversion is as follows :

$$\frac{R(X,T)}{C_0} = (K_1 + K_2 X^m)(1-X)^n \tag{C.1}$$

where C_0 is the initial concentration of reactive species, X denotes the extent of reaction. The constants K_1, K_2 represent the temperature dependence. K_1, K_2, m and n follow from experiments. Fig. (C.1) shows the reaction rate of epoxy compound as a function of time at various temperatures. Experimental values aswell as predictions are presented.
To describe the dynamic viscosity the folllowing equation is proposed :

$$\eta(X,T,\mathbf{D}) = A_\eta(X) exp(\frac{E_\eta(X)}{RT})(2\mathbf{D}:\mathbf{D})^{\frac{n(X)}{2}} \tag{C.2}$$

where R is the gas constant, $\mathbf{D}$ is the rate of strain tensor, T is the temperature and $A_\eta(X), E_\eta(X), n(X)$ denote parameters depending on conversion which follow from experiments. Fig. (C.2) shows the dynamic viscosity predicted by the model and obtained from experiments. When the Cox-Merz rule [4] is applied the frequency corresponds to the shear rate and and the model is valid for epoxy in the region between melting and gelpoint.

Appendix D

Listings

D.1 Main program listing

```
      program reaflow
c
c=======================================================================
c     In this program  the instationairy energy, conversion, impuls and
c     mass balances are solved. The modified theta-method is used to
c     approximate the time derivatives. The problem specific parameters
c     are listed in a seperate input file which is read by the main
c     program.
c     Used files :
c      meshoutput           Output of program sepmesh
c      reaflow.dat          Standard input file
c      reaflow.out          Standard output file
c      reaflow.pos          Postscript input file
c      reaflow.sol          Postscript output file
c
c     subroutines called:
c       SEPSTR: Start the program                                  PG 4.3
c       PRESDF: Prescribe boundary conditions                      PG 5.5
c       FILCOF: Fill coefficients                                  PG 5.3
c       SYSTM2: Compute matrices and large vector                  PG 5.1
c       PRINOV: Print array                                        PG 8.6
c       OUTTIM: Write output                                       PG 8.7
c       FINISH: Stop the program                                   PG 2.5
c
c     In array isol is stored :
c                   column(1)  velocity solution
c                   column(2)  temperature solution
c                   column(3)  conversion solution
c                   column(4)  viscosity
c                   column(5)  heat production
c                   column(6)  reaction rate
c
c     In array ivcold is stored :
c                   column(1)  velocity solution at preceding time level
c                   column(2)  temperature solution at preceding time level
c                   column(3)  conversion solution at preceding time level
c                   column(4)  viscosity
```

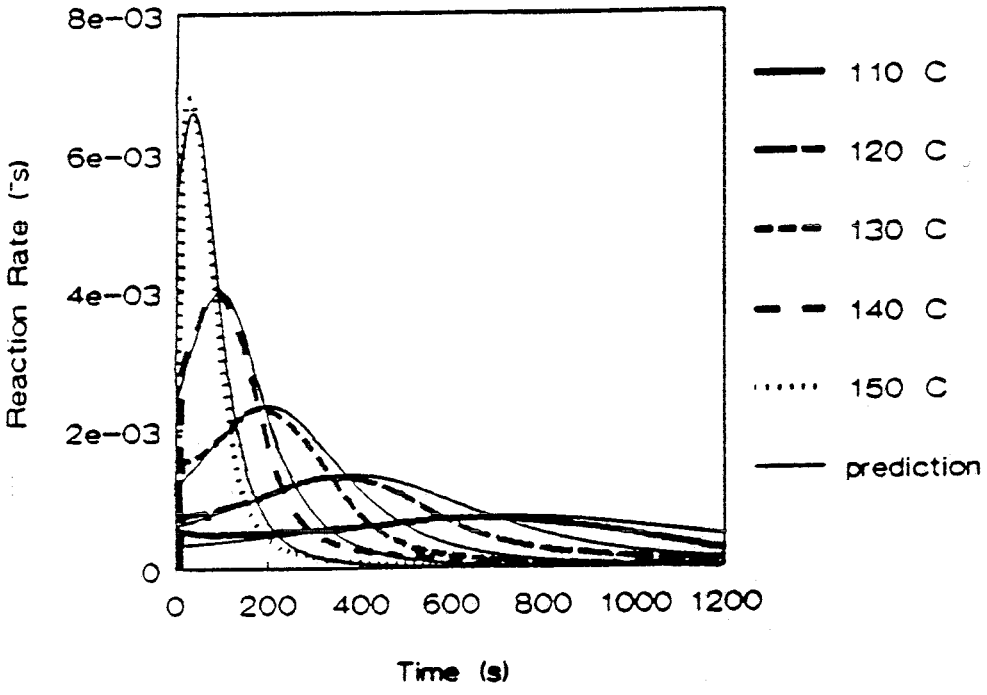

Figure C.1: Measurements and predictions of conversion rate at various temperatures.

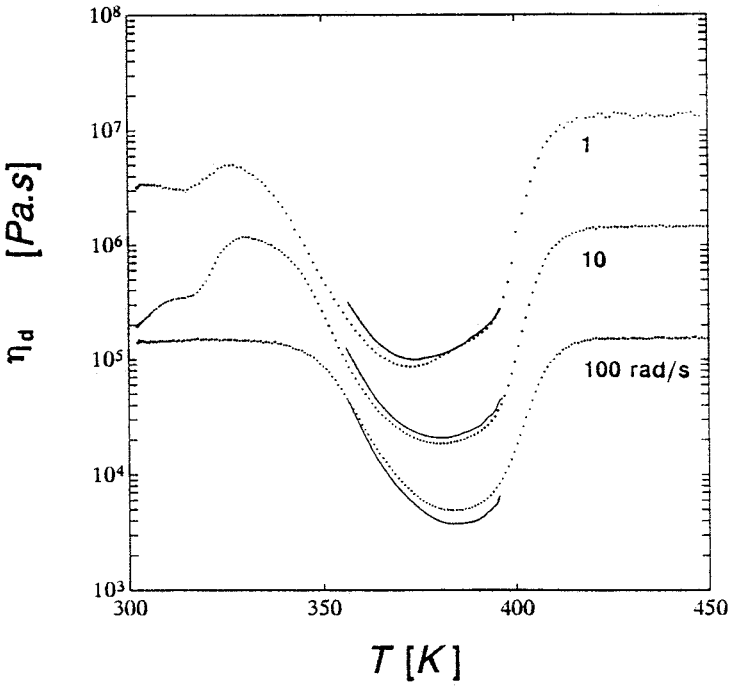

Figure C.2: Measurements and predictions of dynamic viscosity at various frequencies.

```
c                   column(5)  heat production
c                   column(6)  reaction rate
c
c=======================================================================
      implicit none
      double precision values(3)
      double precision difmax1, difmax2, difmax3, tend, p, q
      integer kmesh(100), kprob(300), iuser(100,3), iuserm(100)
      integer matrs(5,3), irhsd(5,3), matrm(5,3)
      integer iessb(5,2), matrms(5,2)
      integer ielhlp, xjdim, jpoint, ipoint
      integer intmat(5,3), isol(5,6), ivcold(5,6), iu1(10)
      integer iinvec(11), invec1(5,3)
      integer invec2(5,3)
      integer ichois, ix, jdegfd, ivec
      integer ivalue, istep, ipress(5)
      integer i, iresul(5,2), ihelp(5,2)
      integer shearv(5), shearn(5), iinder(2), imas
      integer ieta(5), idum(5,3)
      integer itemp(5), iconv(5)
      integer jbuffr, jbfree

      double precision user(100,3), u1(10), alpha2, beta2, userm(100)
      double precision rinvec(11)

      common /cbuffr/ nbuffr, kbuffr, intlen, ibfree
      integer nbuffr, kbuffr, intlen, ibfree
      common /cmcdpi/ irefwr, irefre, irefer
      integer irefwr, irefre, irefer
      common /ctime/ theta, deltat, t, ratime(7),
     .               nstep, irtime(9)
      integer ictime, nstep, irtime
      double precision theta, deltat, t, ratime, tstep
      double precision tmove, tmoved
c
c=======================================================================
c     S T A R T   T H E   P R O G R A M                        PG 4.3
c=======================================================================
      kmesh(1)   = 100
      kprob(1)   = 300
      iuser(1,1) = 100
      user(1,1)  = 100
      iuser(1,2) = 100
      user(1,2)  = 100
      iuser(1,3) = 100
      user(1,3)  = 100
      iuserm(1)  = 100
      userm(1)   = 100
      CALL SEPSTR( kmesh, kprob, intmat )
```

```
c
c=======================================================================
c     C R E A T E   S T A R T   V A L U E S                    PG 5.3
c=======================================================================
      CALL CREATE( 0, kmesh, kprob, ivcold )
      CALL CREATE( 0, kmesh, kprob, isol )
c
c=======================================================================
c     Read parameters :
c                       theta,  parameter in the theta-method.
c                       tend,   time span.
c                       nstep,  number of time steps over tend.
c                       tmove,  time at which boundary conditions are
c                               modified.
c=======================================================================
10    format(' double precision theta=', f10.2 )
      read(*,*) theta
      write(*,20)
20    format(' double precision tend=', f10.2 )
      read(*,*) tend
      write(*,30)
30    format(' integer nstep=', i5 )
      read(*,*) nstep
      write(*,40)
40    format(' double precision tmove=', f10.2 )
      read(*,*) tmove
      write(irefwr,*)'theta:',theta
      write(irefwr,*)'tend:',tend
      write(irefwr,*)'nstep:',nstep
      write(irefwr,*)'tmove:',tmove

      deltat = tend/nstep
      t = 0d0
c
c=======================================================================
c     S T A R T   I T E R A T I O N
c=======================================================================
      do 500 istep = 1,nstep
      write(irefwr,*)'istep:',istep
      tstep = theta*deltat
      tmoved = tmove + tstep
      t = t + tstep
```

```
c
c=======================================================================
c     P R E S C R I B E   B O U N D A R Y   C O N D I T I O N S  PG 5.5
c=======================================================================
      if ( istep.eq.1 ) then
          CALL PRESDF( kmesh, kprob, isol )
      else if ( t.ge.tmove )  then
            if ( t.lt.tmoved )  then
                CALL PRESDF( kmesh, kprob, isol )
            endif
      endif
c
c=======================================================================
c     F I L L   C O E F F I C I E N T S                      PG 5.11
c=======================================================================
      if ( istep.eq.1 ) then
          CALL FILCOF( iuser(1,1), user(1,1), kprob, kmesh, 1 )
      endif
      CALL COPYVC( isol(1,1), ivcold(1,1) )
      CALL COPYVC( isol(1,2), ivcold(1,2) )
      CALL COPYVC( isol(1,3), ivcold(1,3) )
c
c=======================================================================
c     I M P U L S  E Q U A T I O N
c     Solve the instationary impuls, mass equations at t(n+theta)
c=======================================================================
c
c=======================================================================
c     C O M P U T E  M A T R I C E S  &  V E C T O R        PG 5.1
c=======================================================================
      CALL SYSTM2( -1, 1, 1, matrs(1,1), intmat(1,1), kmesh,
     &             kprob, irhsd(1,1),matrm(1,1), isol(1,1),
     &             iuser(1,1), user(1,1), 6, ivcold, ielhlp )
c
c=======================================================================
c     S O L V E   E Q U A T I O N                            PG 6.8
c=======================================================================
      CALL SOLVE( 1, matrs(1,1), isol(1,1), irhsd(1,1), intmat(1,1),
     &            kprob )
c
c=======================================================================
c     H E A T   E Q U A T I O N
c     Solve the instationary temperature equation at t(n+theta)
c=======================================================================
c
c
c=======================================================================
c     C O M P U T E  M A T R I X  &  V E C T O R            PG 5.1
c     compute stiffness matrix
c     and right-hand side without essential boundary
c     conditions
c=======================================================================
```

```
      if ( istep.eq.1 ) then
          CALL FILCOF( iuser(1,2), user(1,2), kprob, kmesh, 2 )
      endif
      CALL SYSTM2( -11, 0, 2, matrs(1,2), intmat(1,2), kmesh,
     &             kprob, irhsd(1,2), idum(1,2), isol(1,2),
     &             iuser(1,2), user(1,2), 6, ivcold, ielhlp )
c
c=======================================================================
c     C O M P U T E  M A T R I X                                PG 5.1
c     compute non-diagonal mass matrix
c=======================================================================
      if ( istep.eq.1 ) then

        CALL CHTYPE(1002,kprob)
        CALL SYSTM2( 14, 0, 2, matrm(1,2), intmat(1,2), kmesh,
     &               kprob, irhsd(1,2), idum(1,2), isol(1,2),
     &               iuser(1,2), user(1,2), 6, ivcold, ielhlp )
        CALL CHTYPE(1001,kprob)
      endif
c
c=== compute mass matrix * old temperature ================== PG 6.9 =
c
      CALL MAVER( matrm(1,2), ivcold(1,2), iresul(1,1), intmat(1,2),
     &            kprob, 4 )
c
c=== add right hand side * tstep ============================ PG 6.5 =
c
      CALL ALGEBR( 3, 0, iresul(1,1), irhsd(1,2), ihelp(1,1),
     &             kmesh, kprob, 1d0, tstep, p, q, ipoint )
c
c=== create new large matrix ================================ PG 5.10=
c
      CALL COPYMT( matrs(1,2), matrms(1,1), kprob )
      CALL ADDMAT( kprob, matrms(1,1), matrm(1,2), intmat(1,2), tstep,
     &             alpha2, 1d0, beta2 )
c
c=== boundaries at new time level ======================================
c
      CALL MAVER( matrms(1,1), isol(1,2), iessb(1,1), intmat(1,2),
     &            kprob, 6 )
      CALL ALGEBR( 3, 0, ihelp(1,1), iessb(1,1), iresul(1,1),
     &             kmesh, kprob, 1d0, -1d0, p, q, ipoint )
c
c=======================================================================
c     S O L V E   E Q U A T I O N                               PG 6.8
c=======================================================================
      CALL SOLVE( 0, matrms(1,1), isol(1,2), iresul(1,1), intmat(1,2),
     &            kprob )
c
c=======================================================================
c     C O N V E R S I O N   E Q U A T I O N
c     Solve the instationary conversion equation at t(n+theta)
c=======================================================================
```

```
c
c
c=======================================================================
c     C O M P U T E  M A T R I X  &  V E C T O R              PG 5.1
c     compute stiffness matrix
c     and right-hand side without essential boundary
c     conditions
c=======================================================================
      if ( istep.eq.1 ) then
          CALL FILCOF( iuser(1,3), user(1,3), kprob, kmesh, 3 )
      endif
      CALL SYSTM2( -11, 0, 3, matrs(1,3), intmat(1,3), kmesh,
     &             kprob, irhsd(1,3), idum(1,3), isol(1,3),
     &             iuser(1,3), user(1,3), 6, ivcold, ielhlp )
c
c=======================================================================
c    C O M P U T E   M A S S - M A T R I X
c    Compute non-diagonal mass matrix
c=======================================================================
      if ( istep.eq.1 ) then
        CALL CHTYPE(2002,kprob)
        CALL FILCOF( iuserm(1), userm(1), kprob, kmesh, 3 )
        CALL SYSTM2( 14, 0, 3, matrm(1,3), intmat(1,3), kmesh,
     &               kprob, irhsd(1,3), idum(1,3), isol(1,3),
     &               iuserm(1), userm(1), 6, ivcold, ielhlp )
        CALL CHTYPE(2001,kprob)
      endif
c
c=== compute mass matrix * old conversion ===================== PG 6.9 =
c
      CALL MAVER( matrm(1,3), ivcold(1,3), iresul(1,2), intmat(1,3),
     &            kprob, 4 )
c
c=== add right hand side * tstep ============================== PG 6.5 =
c
      CALL ALGEBR( 3, 0, iresul(1,2), irhsd(1,3), ihelp(1,2),
     &             kmesh, kprob, 1d0, tstep, p, q, ipoint )
c
c=== create new large matrix ================================== PG 5.10
c
      CALL COPYMT( matrs(1,3), matrms(1,2), kprob )
      CALL ADDMAT( kprob, matrms(1,2), matrm(1,3), intmat(1,3),
     &             tstep, alpha2, 1d0, beta2 )
c
c=== boundaries at new time level ===================================
c
      CALL MAVER( matrms(1,2), isol(1,3), iessb(1,2), intmat(1,3),
     &            kprob, 6 )
      CALL ALGEBR( 3, 0, ihelp(1,2), iessb(1,2), iresul(1,2),
     &             kmesh, kprob, 1d0, -1d0, p, q, ipoint )
```

```
c
c=======================================================================
c     S O L V E   E Q U A T I O N                              PG 6.8
c=======================================================================
      CALL SOLVE( 0, matrms(1,2), isol(1,3), iresul(1,2), intmat(1,3),
     &            kprob )
c
c=======================================================================
c     C O M P U T E   S O L U T I O N  A T  T ( N + 1 )        PG 6.5
c=======================================================================
      CALL ALGEBR( 3, 0, isol(1,1), ivcold(1,1), isol(1,1), kmesh,
     &             kprob, 1d0/theta, (theta-1d0)/theta, p, q, ipoint )
      CALL DIFFVC( 0, isol(1,1), ivcold(1,1), kprob, difmax1 )
      write(6,2000) istep,difmax1

      CALL ALGEBR( 3, 0, isol(1,2), ivcold(1,2), isol(1,2), kmesh,
     &             kprob, 1d0/theta, (theta-1d0)/theta, p, q, ipoint )
      CALL DIFFVC( 0, isol(1,2), ivcold(1,2), kprob, difmax2 )
      write(6,2100) istep,difmax2

      CALL ALGEBR( 3, 0, isol(1,3), ivcold(1,3), isol(1,3), kmesh,
     &             kprob, 1d0/theta, (theta-1d0)/theta, p, q, ipoint )
      CALL DIFFVC( 0, isol(1,3), ivcold(1,3), kprob, difmax3 )
      write(6,2200) istep,difmax3

      t = t + (1d0 - theta)*deltat

c
c=======================================================================
c     C O M P U T E   S H E A R   R A T E                      PG 5.4
c     There appears to be a bug in DERIVA. In order to overwrite
c     the computed shear rate vector, INI056 is called.
c=======================================================================
      ichois = 600
      if ( istep. gt. 1 ) then
         CALL INI056(shearv,'Main')
         kbuffr = jbuffr
         ibfree = jbfree
      endif
      CALL DERIVA( ichois, 9, ix, jdegfd, ivec, shearv, kmesh,
     &             kprob, isol, isol, iuser, user, ielhlp )
c
c=======================================================================
c     The shear rate is only computed in the vertices of the element.
c     To interpolate these values to nodal points, DERIV is called.
c=======================================================================
      iinder(1) = 2
      iinder(2) = 4
      CALL DERIV( iinder, shearn, kmesh, kprob, shearv,
     &            iuser(1,1), user(1,1) )
```

```
c
c=======================================================================
c     In order to manipulate the shear rate, temperature and conversion
c     solutions, these vectors have to be of exactly the same structure.
c     To accomplish this, the temperature and conversion are remapped to
c     problem 1 and treated as vectors of special structure instead of
c     solution vectors.
c=======================================================================
      iinvec(1) = 11
      iinvec(2) = 51
      iinvec(5) = 2
      iinvec(11)= 1

      CALL MANVEC( iinvec, rinvec, isol(1,2), isol, itemp,
     &             kmesh, kprob )
      CALL MANVEC( iinvec, rinvec, isol(1,3), isol, iconv,
     &             kmesh, kprob )
c
c**** fill array invec1 with shear rate, temperature and conversion ****
c
      do 150 i=1,5
         invec1(i,1) = shearn(i)
         invec1(i,2) = itemp(i)
         invec1(i,3) = iconv(i)
150   continue
c
c=======================================================================
c     C O M P U T E   E T A                                    PG 6.5
c=======================================================================
      iinvec(1) = 11
      iinvec(2) = 32
      iinvec(5) = 3
      rinvec(1) = 3d0
      CALL MANVEC( iinvec, rinvec, invec1, invec2, ieta,
     &             kmesh, kprob )
c
c=======================================================================
c     Due to large viscosity gradients ,it is possible that the
c     viscosity in the centroid of the element obtains a negative
c     value. To avoid this, the viscosity values in the vertices of the
c     elements is interpolated lineairly to the nodal points.
c=======================================================================
      iinder(1) = 2
      iinder(2) = 4
      CALL DERIV( iinder, ivcold(1,4), kmesh, kprob, ieta,
     &            iuser(1,1), user(1,1) )
      if (istep.eq.nstep) then
       CALL PRINOV( ivcold(1,4), kmesh, kprob, 1, 'output deriv :
     &              ivcold(1,4)', xjdim, jpoint )
      endif
```

```
c
c=======================================================================
c     C O M P U T E  V I S C O U S  D I S S I P A T I O N        PG 6.5
c=======================================================================
      rinvec(1) = 2d0
      CALL MANVEC( iinvec, rinvec, invec1, invec2, ivcold(1,5),
     &             kmesh, kprob )
c
c=======================================================================
c     C O M P U T E   R E A C T I O N   R A T E                  PG 6.5
c=======================================================================
      rinvec(1) = 1d0
      CALL MANVEC( iinvec, rinvec, invec1, invec2, ivcold(1,6),
     &             kmesh, kprob )
c
c=======================================================================
c     W R I T E   O U T P U T                                    PG 8.7
c=======================================================================
      CALL COPYVC( ivcold(1,4), isol(1,4) )
      CALL COPYVC( ivcold(1,5), isol(1,5) )
      CALL COPYVC( ivcold(1,6), isol(1,6) )
      if ( mod(istep,50).eq.1.or.t.ge.tmove ) then
          CALL OUTTIM( t, kmesh, kprob, isol )
      endif
c
c==== continue computation ============================================
c
      write(6,2300) t
      if ( istep. eq. 1 ) then
         jbuffr = kbuffr
         jbfree = ibfree
      endif
500   continue
      write(*,*) 501
c
c=======================================================================
c     S T O P   T H E   P R O G R A M                            PG 4.3
c=======================================================================
      CALL FINISH( 0 )

2000  format( ' istep: ',i5,' difmax1 = ',e10.3 )
2100  format( ' istep: ',i5,' difmax2 = ',e10.3 )
2200  format( ' istep: ',i5,' difmax3 = ',e10.3 )
2300  format( ' time= ',e10.3 )
      end
c
c%%%%%%%%%%%%%%%%%%%%%%%%%%%%%%%%%%%%%%%%%%%%%%%%%%%%%%%%%%%%%%%%%%%%%%%%%%
c
c
```

```
c*********************************************************************
c     Compute properties as a function of old solutions
c     reavec(1)=shear rate, reavec(2)=temperature, reavec(3)=conversion
c*********************************************************************
c
      SUBROUTINE FUNVEC( rinvec, reavec, nvec, coor, outvec )
      integer nvec
      double precision rinvec(*), reavec(nvec), coor(*), outvec
      double precision K1, K2, n, m
      double precision X1, X2, X3, X4, X5, X6, X7, X8, X9
      double precision Er, lnA, lneta, eta, nx, Xg, R, Hr
      Xg = 1.8d-1
      Hr = -9d7
      reavec(1)=abs(reavec(1))
      reavec(2)=abs(reavec(2))
c
c**** prevent negative conversion to increase ***************************
c
      if (reavec(3).lt.0d0) then
         reavec(3)=0d0
      endif
      if (reavec(3).gt.1d0) then
         reavec(3)=1d0
      endif
       if (rinvec(1).lt.2.5d0) then
c
c**** determine reaction rate of conversion *********************************
c
           K1 = 1.18d6*exp(-8.43d3/reavec(2))
           K2 = 4.71d7*exp(-8.91d3/reavec(2))
            n = 1.38d0
            m = 1.24d0
            R = (K1 + K2*(reavec(3)**m))*(1d0 - reavec(3))**n
       endif
       if (rinvec(1).gt.1.5d0) then
c
c**** detetmine dynamic viscosity ******************************************
c
           X1 = reavec(3)
            if (X1.gt.Xg) then
                eta = 1d7
            else
                   X2 = X1*X1
                   X3 = X2*X1
                   X4 = X3*X1
                   X5 = X4*X1
                   X6 = X5*X1
                   X7 = X6*X1
                   X8 = X7*X1
                   X9 = X8*X1
```

```
                lnA = -6.8245114d10*X9 + 6.7661336d10*X8
     .                -2.8783190d10*X7 + 6.8086308d9*X6
     .                -9.6881378d8*X5  + 8.3393625d7*X4
     .                -4.0754728d6*X3  + 8.8251837d4*X2
     .                +5.0830918d2*X1  - 4.1139134d1
                  Er =  2.3105185d13*X9 - 2.3188884d13*X8
     .                +9.9903682d12*X7 - 2.3930239d12*X6
     .                +3.4461300d11*X5 - 2.9999969d10*X4
     .                +1.4824887d9*X3  - 3.2610199d7*X2
     .                -1.6831220d5*X1  + 1.9143169d4
                  nx = -1.9015740d9*X9  + 1.6151901d9*X8
     .                -5.7894979d8*X7  + 1.1391361d8*X6
     .                -1.3413323d7*X5  + 9.6929725d5*X4
     .                -4.2945433d4*X3  + 1.2054279d3*X2
     .                -2.7358233d1*X1  - 2.3518698d-1

                lneta=lnA + Er/reavec(2)
c
c**** set minimum shear rate ************************************************
c
                eta=(exp(lneta))*((reavec(1)+1d-2)**nx)
             endif
          endif

             if (rinvec(1).lt.1.5d0) then
c
c**** write reaction rate ****************************************************
c
                 outvec = R
             else



               if (rinvec(1).lt.2.5d0) then
c
c**** write viscous dissipation **********************************************
c
                   outvec = eta*(reavec(1))**2d0 - Hr*R
               else
                  if (rinvec(1).lt.3.5d0) then
c
c**** write dynamic viscosity ************************************************
c
                      outvec = eta
                  endif
               endif
             endif
       end
```

D.2 Input file listing

```
*
* === INPUT FOR "reaflow"================================ SEPSTR/START/MESHRD
*
set warn on                                  # display warnings (on/off)
set time on                                  # display CPU time (off/on)
set output on                                # display all information (off/on/out)
start
   database = not                            # use file2 (not/new/old)
   norotate                                  # rotate plots (norotate/rotate)
   renumber sloan band                       # renumber
   sepcomp = formatted                       # file format for sepcomp.out
end
*
* === INPUT FOR "reaflow"============================== PG 4.1 = SEPSTR/PROBDF
*
problem 1
   types
      elgrp1=400                             # Type number for Navier Stokes
   essbouncond                               # Carthesian coordinates
      degfd1=curves0(c1,c12)
      degfd2=curves0(c1,c9)
problem 2
   types
      elgrl1=(104,509)                       # Type numbers for heat equation
   essbouncond
      degfd1=curves0(c3,c7)
problem 3
   types
      elgrl1=(124,509)                       # Type numbers for conversion equation
end
*
* === INPUT FOR "reaflow"============================== PG 4.4 = SEPSTR/COMMAT
*
matrix
   method = 2, problem = 1                   # Non-symmetrical profile matrix
   method = 2, problem = 2                   # Non-symmetrical profile matrix
   method = 2, problem = 3                   # Non-symmetrical profile matrix
end
*
* === INPUT FOR "reaflow"============================== PG 5.3 ======= CREATE
*
*
create vector 4, problem 1                 # Fill array ivcold
   type = vector of special structure 2
   value = 1d3
create vector 5, problem 1
   type = vector of special structure 2
   value = 0d0
create vector 6, problem 1
   type = vector of special structure 2
   value = 0d0
end
```

```
create vector 1, problem 1                    # Fill array isol
   type = solution vector
   value = 0d0
create vector 2, problem 2
   type = solution vector
   value = 2.93d2
create vector 3, problem 3
   type = solution vector
   value = 0d0
create vector 4, problem 1
   type = vector of special structure 2
   value = 1d3
create vector 5, problem 1
   type = vector of special structure 2
   value = 0d0
create vector 6, problem 1
   type = vector of special structure 2
   value = 0d0
end
*
*
* === INPUT FOR "reaflow"================================ PG 5.5 ======== PRESDF
*
essential boundary conditions 1
   curves0(c1),degfd1,degfd2=(value=0d0)
   curves0(c2),degfd1,degfd2=(value=0d0)
   curves0(c8),degfd1,degfd2=(value=0d0)
   curves0(c9),degfd1,degfd2=(value=0d0)
   curves0(c3),degfd1=(value=0d0)
   curves0(c4),degfd1=(value=0d0)
   curves0(c5),degfd1=(value=0d0)
   curves0(c6),degfd1=(value=0d0)
   curves0(c7),degfd1=(value=0d0)
   curves0(c3),degfd2=(value=0d0)          # Zero velocity at wall.
   curves0(c4),degfd2=(value=0d0)
   curves0(c5),degfd2=(value=0d0)
   curves0(c6),degfd2=(value=0d0)
   curves0(c7),degfd2=(value=0d0)
essential boundary conditions 2
   curves0(c3),degfd1=(value=3.84d2)
   curves0(c4),degfd1=(value=3.84d2)
   curves0(c5),degfd1=(value=3.84d2)
   curves0(c6),degfd1=(value=3.84d2)
   curves0(c7),degfd1=(value=3.84d2)
end
*
* === INPUT FOR "reaflow"================================ PG 5.11 ======= FILCOF
*
```

```
*  Definition of coefficients for impuls equation
coefficients 1
   elgrp1 ( nparm=8 )          # The coefficients are defined by 8 parameters
      coef1  =(value=1d-8)     #  1:  Penalty function parameter eps
      coef2  =(value=1.8d3)    #  2:  Density
      icoef3 =10               #  3:  Type of linearization (10=Stokes flow)
                               #                            (11=Picard)
                               #                            (12=Newton)
                               #  4:  angular velocity = 0
                               #  5:  body force in x-direction = 0
                               #  6:  body force in y-direction = 0
      icoef7 =1                #  7:  type of constitutive equation (1=Newtonian
                               #                                     (2=powerlaw
      coef8  =(old solution 4)
                               #  8:  eta
end
*  Definition of coefficients for heat equation
coefficients 2
   elgrp1 ( nparm=8 )          # The coefficients are defined by 8 parameters
      coef1 =(value=3d-1)      # 1: a11 =heat conductivity
                               # 2: a12
      coef3 =(value=3d-1)      # 3: a22 =heat conductivity
      coef4 =(old solution 1, degree of freedom 1, coef=2.16d6 )
                               # 4: radial velocity
      coef5 =(old solution 1, degree of freedom 2, coef=2.16d6 )
                               # 5: axial velocity
                               # 6: beta
      coef7 =(old solution 5, coef=1d0)
                               # 7: heat source
      coef8 =(value=2.16d6)    # 8: density*heat capacity
end
* Definition of coefficients for conversion equation
coefficients 3
   elgrp1 ( nparm=8 )          # The coefficients are defined by 8 parameters
      coef1 =(value=0d0 )      # 1: a11 =diffusion
                               # 2: a12
      coef3 =(value=1d-15)     # 3: a22 =diffusion
      coef4 =(old solution 1, degree of freedom 1)
                               # 4: radial velocity
      coef5 =(old solution 1, degree of freedom 2)
                               # 5: axial velocity
                               # 6: beta
      coef7 =(old solution 6, coef=1d0)
                               # 7: right hand side
      icoef8= 1                # 8: coefficient for streamline upwinding
end
coefficients 3
   elgrp1 ( nparm=8 )          # The coefficients are defined by 8 parameters
      coef8=(value=1d0)        # 8: coefficient in front of mass matrix
end
```

```
*
* === INPUT FOR "reaflow"================================================ OUTPUT
*
output
write 6 solutions
end
*
* === INPUT FOR "reaflow"============================== PG 5.5 ======== PRESDF
*
essential boundary conditions 1
   curves0(c1),degfd1,degfd2=(value=0d0)
   curves0(c2),degfd1,degfd2=(value=0d0)
   curves0(c8),degfd1,degfd2=(value=0d0)
   curves0(c9),degfd1,degfd2=(value=0d0)
   curves0(c3),degfd1=(value=0d0)
   curves0(c4),degfd1=(value=0d0)
   curves0(c5),degfd1=(value=0d0)
   curves0(c6),degfd1=(value=0d0)
   curves0(c7),degfd1=(value=0d0)
   curves0(c3),degfd2=(value=2.5d-3)
   curves0(c4),degfd2=(value=2.5d-3)
   curves0(c5),degfd2=(value=2.5d-3)
   curves0(c6),degfd2=(value=2.5d-3)
   curves0(c7),degfd2=(value=2.5d-3)
essential boundary conditions 2
   curves0(c3),degfd1=(value=3.84d2)
   curves0(c4),degfd1=(value=3.84d2)
   curves0(c5),degfd1=(value=3.84d2)
   curves0(c6),degfd1=(value=3.84d2)
   curves0(c7),degfd1=(value=3.84d2)
end
```

D.3 Mesh listing

```
mesh2d
points
p1 =(0,0)
p2 =(6d-3,0)
p3 =(8d-3,0)
p4 =(8d-3,2d-3)
p5 =(8d-3,8d-3)
p6 =(8d-3,5.2d-2)
p7 =(8d-3,5.8d-2)
p8 =(8d-3,6d-2)
p9 =(6d-3,6d-2)
p10=(0,6d-2)
p11=(0,5.2d-2)
p12=(0,8d-3)
p13=(6d-3,2d-3)
p14=(6d-3,5.8d-2)
curves
c1 =line2(p1, p2,nelm=5,ratio=1,factor=.25)
c2 =line2(p2, p3,nelm=5,ratio=1,factor=.25)
c3 =line2(p3, p4,nelm=5,ratio=1,factor=4)
c4 =line2(p4, p5,nelm=5,ratio=1,factor=4)
c5 =line2(p5, p6,nelm=16,ratio=0,factor=0)
c6 =line2(p6, p7,nelm=5,ratio=1,factor=.25)
c7 =line2(p7, p8,nelm=5,ratio=1,factor=.25)
c8 =line2(p8, p9,nelm=5,ratio=1,factor=4)
c9 =line2(p9,p10,nelm=5,ratio=1,factor=4)
c10=line2(p10,p11,nelm=5,ratio=1,factor=4)
c11=line2(p11,p12,nelm=16,ratio=0,factor=0)
c12=line2(p12,p1,nelm=5,ratio=1,factor=.25)
c13=line2(p4,p13,nelm=5,ratio=1,factor=4)
c14=line2(p13,p2,nelm=5,ratio=1,factor=.25)
c15=line2(p9,p14,nelm=5,ratio=1,factor=4)
c16=line2(p14,p7,nelm=5,ratio=1,factor=.25)
c17=line2(p5,p12,nelm=5,ratio=1,factor=4)
c18=line2(p11,p6,nelm=5,ratio=1,factor=.25)
c19=line2(p13,p12,nelm=5,ratio=1,factor=4)
c20=line2(p14,p11,nelm=5,ratio=1,factor=4)
surfaces
s1=rectangle4(5,5,c1,-c14,c19,c12)
s2=rectangle4(5,5,c2,c3,c13,c14)
s3=rectangle4(5,5,c4,c17,-c19,-c13)
s4=rectangle4(16,5,c5,-c18,c11,-c17)
s5=rectangle4(5,5,c6,-c16,c20,c18)
s6=rectangle4(5,5,c7,c8,c15,c16)
s7=rectangle4(5,5,-c15,c9,c10,-c20)
meshsurf
selm1=(s1,s7)
plot(yfact=0.2)
renumber
end
```

D.4 Post process file listing

```
set warn on                                    # display warnings (on/off)
set time on                                    # display CPU time (off/on)
set output on                                  # display all information (off/on/out)
start
   database = not                              # use file2 (not/new/old)
   norotate                                    # rotate plots (norotate/rotate)
   renumber sloan band                         # renumber
   sepcomp = formatted                         # file format for sepcomp.out
end
postprocessing
time=(308)
name v0=velocity
name v1=temperature
name v2=conversion
name v3=dynamic viscosity
name v4=viscous dissipation
name v5=reaction rate
compute v6 = intersection v0, degfd=2, origin=(0,2d-3), angle=0
compute v7 = intersection v0, degfd=2, origin=(0,3d-2), angle=0
compute v8 = intersection v1, degfd=1, origin=(0,3.0d-2), angle=0
compute v9 = intersection v2, degfd=1, origin=(0,3.0d-2), angle=0
compute v10 = intersection v0, degfd=1, origin=(4d-3,0), angle=90
compute v11 = intersection v1, degfd=1, origin=(4d-3,0), angle=90
compute v12 = intersection v2, degfd=1, origin=(4d-3,0), angle=90
plot function v6, textx='r', texty='axial velocity', steps=(8,10)
plot function v7, textx='r', texty='axial velocity', steps=(8,10)
plot function v8, textx='r', texty='temperature',steps=(8,10)
plot function v9, textx='r', texty='conversion',steps=(8,10)
plot function v10,textx='z', texty='radial velocity'
plot function v11,textx='z', texty='temperature'
plot function v12,textx='z', texty='conversion'
plot vector v0, yfact=0.2, factor=4
plot contour v1, yfact=0.2
plot contour v2, yfact=0.2
plot contour v3, yfact=0.2
#plot contour v4, yfact=0.2
plot contour v5, yfact=0.2

end
```

Appendix E

Viscous heating

E.1 Flow in a circular die with viscous heating

In order to test the uncoupling procedure for the determination of the rigth-hand-sides of the balance equations, a flow problem described in [1] is solved. The example describes viscous heating in a straigth circular tube. The viscosity is assumed to be temperature independent. No chemical reaction takes place.

A melt governed by a power-law equation given by :

$$\eta = mII^{\frac{n-1}{2}} \tag{E.1}$$

where $\sqrt{II}$ is the shear rate and with m and n independent of temperature, enters a circular die at temperature T_0. The die has a radius R and length L.

$$\begin{aligned} R &= 3.94 * 10^{-4}[m] \\ L &= 1.28 * 10^{-2}[m] \\ T_w &= T_0 = 463[K] \end{aligned}$$

The velocity profile at the die entrance is fully developed. Density, heat capacity and thermal conductivity are independent of pressure and temperature. The die wall is maintained at temperature T_w. The melt has the following physical properties :

$$\begin{aligned} \rho &= 1.8 * 10^3[\frac{kg}{m^3}] \\ C_p &= 10^3[\frac{J}{kg\,K}] \\ \lambda &= 2.5 * 10^{-1}[\frac{W}{mK}] \\ n &= 0.5[-] \\ m &= 6.9 * 10^3[Pa\sqrt{s}] \end{aligned}$$

It is convenient to rewrite the equations of motion and energy in dimensionless form by introducing the following dimensionless quantities :

$$\xi = \frac{r}{R}$$
$$\zeta = \frac{\alpha z}{v_{max} R^2}$$
$$\theta = \frac{(T - T_0)\lambda}{mR^2(\frac{v_{max}}{R})^{1.5}}$$

The mathematical problem to be solved becomes :

$$(1 - \xi^3)\frac{\partial \theta}{\partial \zeta} = \frac{\partial}{\xi \partial \xi}(\xi \frac{\partial \theta}{\partial \xi}) + 5.2\,\zeta^3 \tag{E.2}$$

with boundary conditions :

$$\zeta = 0 \Rightarrow \theta = 0 \tag{E.3}$$
$$\xi = 0 \Rightarrow \frac{\partial \theta}{\partial \xi} = 0 \tag{E.4}$$
$$\xi = 1 \Rightarrow \theta = 0 \tag{E.5}$$

The solution of this problem is split into two parts ; a solution for very large ζ and a function that cancels the solution at $\zeta = 0$ and which tends to zero for very large ζ. This will eventually give an eigenvalue problem. With the solution of this problem we obtain the temperature distribution in the die. For details see [1].

E.2 Numerical procedure

The equation of motion and energy are coupled by convection and dissipation. The equations are solved iteratively, the momentum equations and the temperature equation are solved simultaneously ; in Sepran terms [10] this is called "coupled".
The iterative procedure is as follows :

1. Start with an approximation of velocity and temperature, being the solution of the Stokes equation aswell as the energy equation without convective terms. To ensure a stable temperature development and rapid convergence of the solution, start with a viscosity which is 10^{-2} times the real value.
2. Compute the solution of the system of equations with first Newton and second Picard linearization [10]. Set the viscosity to the real value.
3. Repeat step 2 until convergence has been achieved.

E.3 Numerical results

The results are shown in fig.(1) of the article. The temperature profiles illustrate how the temperature increases from the value at the entrance to a maximum at the tube end. At the wall the entrance temperature is maintained. Because of viscous dissipation

there's a peak in temperature. The maximum shear rate is at the wall. Because of the constant wall temperature, the temperature peak will arise near the wall. Due to the low thermal conductivity of the melt, the centre-tube-temperature will slowly increase and therefore the temperature peak will move to the centre of the tube.
The maximum computed dimensionless temperature T^*_{max}, is 0.117. In the example this value is 0.12. As may be seen from fig.(1), the numerical solution of this problem compares well with the solution from the example [1]. The real temperature rise is $2.4[K]$. So if we were to look at a physical problem the independency of the viscosity and temperature would no longer be acceptable.

Bibliography

[1] R.B. Bird, R.C. Armstrong and O. Hassager. *Dynamics of polymeric liquids 1987*

[2] R.B. Bird, W.E. Stewart and E.N. Lightfoot. *Transport phenomena, 1960.*

[3] A.N. Brooks and T.J.R. Hughes. *Comp.Meth.Appl.Mech.and Eng., 32 1982*

[4] W.P. Cox and E.H. Merz. *J.Polym.Sci., 28 1958*

[5] J.B. Enns and J.K. Gillham. *J.Appl.Pol.Sci., 28 1983*

[6] A.I. Isayev. *Injection and compression molding fundamentals, 1987*

[7] M.R. Kamal and S. Sourour. *Polym.Eng.Sci., 13:41 1976* and *Thermoch.Acta, 14:41 1976*

[8] S.P. Parker. *FLuid mechanics source book, 1988.*

[9] J.R.A Pearson. *Polymer flows dominated by high heat generation and low heat transfer, Pol. Eng. Sci. 18:3 1978.*

[10] A. Segal. *Sepran manual*

[11] A.B. Spoelstra and J.M.M. Kok. *TUE report, WFW 91.059 1991*